Received: 16 February 2020 | Revised: 10 May 2020 | Accepted: 18 May 2020

DOI: 10.1111/ijac.13567

ORIGINAL ARTICLE

International Journal of Applied Ceramic TECHNOLOGY

Review: Effect on physical, mechanical, and wear performance of ZrB_2-based composites processed with or without additives

Vikas Verma[1] | **Vladimir Cheverikin**[1] | **Ronaldo Câmara Cozza**[2]

[1]Thermochemistry of Materials SRC, National University of Science and Technology (NUST) MISiS, Moscow, Russia

[2]Department of Mechanical Engineering, University Center FEI, São Bernardo do Campo, Brazil

Correspondence
Vikas Verma, Thermochemistry of Materials SRC, National University of Science and Technology (NUST) MISiS, Moscow, Russia.
Email: vikasverma.iitr@rediffmail.com

Funding information
Ministry of Science and Higher Education of the Russian Federation in the framework of Increase Competitiveness Program of NUST «MISiS» (№ K4-2018-020), implemented by a governmental decree dated 16th of March 2013, N 211., Grant/Award Number: K4-2018-020 and B100-D20-2018/0137; Ministry of Science and Higher Education of the Russian Federation, Grant/Award Number: K4-2018-020

Abstract

Because of unique combination of properties, ultra high temperature ceramics (UHTCs) are considered the most suitable material for applications in extreme environments as in hypersonic flights, atmospheric reentry, and rocket propulsion system. Processing of UHTCs especially ZrB_2-based ceramic composites with additives offer advantages in terms of simple processing methodology and excellent properties. Processing route highly controls the ceramic properties. Present review share out systematically and explain the processing strategies of ZrB_2-based ceramic composites—conventional, hot press or spark plasma sintering and their effect on microstructure features, physical, and mechanical properties and tribological performance. Present review suggests that it is possible to process full dense ZrB_2–SiC ceramic composite with ultrafine or nano size particles via fast sintering technique like spark plasma sintering and gives better mechanical and wear resistant properties.

KEYWORDS

additives, ceramics, composites, conventional, spark plasma, wear

1 | INTRODUCTION

In recent few decades, efforts have been made to develop the materials which can perform and sustain successfully in extreme temperature and pressure.[1] Materials such as nitrides, carbides, and transition metal borides comes in the category of ultra high temperature ceramics (UHTCs) having high resistance to oxidation, high thermal conductivity, and better mechanical properties.[2-6] UHTCs act as Thermal Protection System (TPS) for future reusable reentry vehicles with repeated multiple launches associated with rocket propulsion, hypersonic flight, and atmospheric reentry.[7] UHTCs lie in IV-V group as transitional metal boride and carbide. They can be used at a very high temperature because of having high melting points of more than 3000°C.[7] They are used in liquid propellant rocket motors, supersonic planes, space planes, turbojet parts, thermal structures for space planes, and other space probes, gas turbines combustors cans, brakes, after burners, heat shields, prostheses, fixation plates, thermal insulation, rocket nozzles, etc.[8-11] Figure 1A shows the photograph of X43-A, a reusable hypersonic aerospace vehicle that would utilize UHTC leading edges and control surfaces.[9] Processing of ultra high temperature ceramics for manufacturing aerospace sharp-shaped hot-structures is obtained by electrical discharge machining (EDM) by Monteverde et al (2008).[12] Nevertheless, the properties that have made ceramic materials one of the most desirable engineering materials also hinder their machining characteristics. Ceramic surface machined by EDM process in general contain a damage surface layer as well as cracks, which can be removed either by subsequent ultrasonic or abrasive blasting processes in order to enhance the surface integrity and strength.[13] Among borides, ZrB_2 is

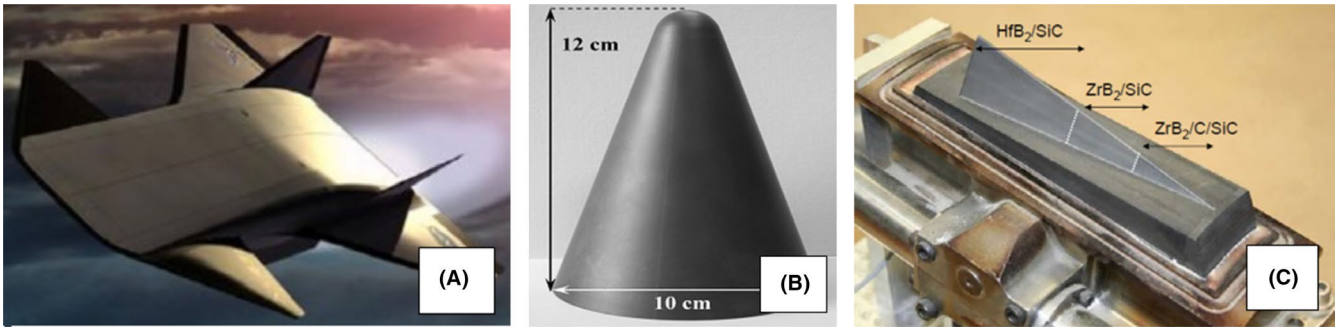

FIGURE 1 A, X43-A, a reusable hypersonic aerospace vehicle that would utilize UHTC leading edges and control surfaces; B, Image courtesy of NASA[9] Hot pressed UHTC nose-cone after shaping by EDM[12]; C, Strakes (composed of three sections, each having a different UHTC composition)[18] [Color figure can be viewed at wileyonlinelibrary.com]

the most promising candidate for leading edge material. It has high oxidation resistance as compared to other borides. UHTC prototype of a nose-cone produced and construction of strakes of space vehicles are shown in Figure 1B,C. Apart from their use in aerothermodynamics for extreme conditions,[14-18] UHTCs are also used in automotive applications as cutting tools, turbine blades, tube vanes, seals, bearings, wear guides, automotive engine components, nozzles, exhaust ducts, heat exchanger tubes, combustors, centrifuges, filters, substrates, air preheaters, wire drawing and extrusion dies, valve seats, high precision balls, bearings, plungers for chemical pumps.[19–21] ZrB_2 and ZrB_2–SiC composites are one of these class of ultra high temperature ceramic composites having incorporating SiC additions making the composite efficient in ultra-refractory properties by enhancing their oxidation resistance and the mechanical properties.[22–24] To increase strength, oxidation resistance, fracture toughness, and to prevent grain growth in ZrB_2 composite, SiC particles are added. SiC having strong covalent bond occur in many different crystal structures, called polytypes.[25–30]

2 | SYNTHESIS AND DEVELOPMENT HISTORY OF ULTRA HIGH-TEMPERATURE CERAMICS

Ultra high temperature ceramics (UHTCs) came into development in 1960s.[1] ZrB_2 has high hardness (>20 GPa), melting temperature (>3000°C), and elastic modulus (~500 GPa); like metals it has high thermal conductivity (60-120 W/m K) and electrical conductivity (21-107 S/m).[1] Therefore, densified ZrB_2-based ceramic composites are preferred for structural applications. Ceramic powders can be synthesized by several chemical, reactive, and reduction processes and ceramic composites can be processed via various processing techniques as conventional sintering, hot press or spark plasma sintering (SPS) for different applications.[31] The simplest reaction for synthesis of zirconium diborides is the elemental precursor powder reaction. However, it limits due to occurrence of exothermic reaction that can melt Zr ZrB_2 can also be synthesized from constituent elements Zr and B by stoichiometric reaction between them via carbothermal and borothermal reduction.[32] ZrB_2 powder can also be obtained by ZrO_2 reduction to its diborides, and by boro/carbo thermal reduction of ZrO_2 (Table 1) in vacuum with B_4C and C addition. At 1650°C, powder mixtures were heated under vacuum in graphite die with 60 minutes isothermal hold, after 60 minutes at 1650°C, argon was filled in furnace and heated at 30°C/min to set sintering temperature. In reaction products, presence of ZrC phase formed gets disappeared with excess amount (20%-25%) of B_4C leaving ZrB_2.[32] Monolithic ceramics properties can be further enhanced with addition of secondary phases. With introduction of secondary phase, the oxidation resistance property of the ceramics can be improved. Second phase as sintering aids form a silica glass protective layer on the surface when surface is exposed to air at high temperature[33-37] as shown in Equations 1 and 2. Sintering aids like $MoSi_2$ or

TABLE 1 Reduction reactions to synthesize ZrB_2 powder[1,32,41-42]

Category	Reaction
Carbothermal	$ZrO_2 + B_2O_3 + 5C \rightarrow ZrB_2 + 5CO$
Borothermal	$ZrO_2 + 4B \rightarrow ZrB_2 + B_2O_2$
Aluminothermal	$3ZrO_2 + 3B_2O_3 + 10Al \rightarrow 3ZrB_2 + 5Al_2O_3$
Boro/Carbothermal Reduction	$7ZrO_2 + 5B_4C \rightarrow 7ZrB_2 + 3B_2O_3 + 5CO$
Boro/Carbothermal Reduction	$2ZrO_2 + B_4C + 3C \rightarrow 2ZrB_2 + 4CO$

SiC increased high resistance to oxidation at high temperatures above 1000°C by forming a protective silica layer on the surface.[38,39]

$$MoSi_2\,(s) + (7/2)\,O_2\,(g) \rightarrow 2SiO_2\,(s) + MoO_3\,(s) \quad (1)$$

$$SiC + 3/2O_2\,(g) \rightarrow SiO_2\,(l) + CO\,(g) \quad (2)$$

Though full densification is difficult to achieve via pressureless (conventional) sintering, it is reported that maximum density of ~ 98% can be achieved for monolithic ZrB_2 at 2150°C held for 9 hours.[40] Khanra et al (2003)[41] prepared ultrafine zirconium diboride from raw oxide (ZrO_2) and boric acid (H_3BO_3) by adding reducing agent (Mg) via self-propagating high temperature synthesis (SHS). Solid state combustion process occurs in SHS and exothermic reaction generates chemical energy for the process to take place. Stoichiometric reaction occurs between Zr and Br synthesizing ZrB_2. The only drawback with SHS is that reactions taking place are difficult to control at extreme rapid heating rate, whereas hot pressing attrition milled Zr and B powders at 600°C for 6 hours gives nanoscale (10 nm in size) ZrB_2 [42]. Summarizing it can be said that ceramic powders can be synthesized by reaction and reduction processes via different sintering techniques with selective sintering parameters.[43]

3 | PHYSICAL AND MECHANICAL PROPERTIES OF UHTCS

In last two decades, research has been done to improve the performance of structural ceramics like ZrB_2 and HfB_2 and work continued on nitrides, oxides, and carbides elements of IV-V group.[1] Diborides have high thermal conductivity than carbides and nitrides making them suitable for high thermal applications.[2] UHTCs are generally classified as oxides and non-oxides. Oxide ceramics are less dense with melting temperature up to 2988 K, whereas non-oxide ceramics are denser and have melting temperature ˃3200 K. Strong covalent bond gives stability to UHTCs. ZrB_2 have high melting point (3244°C), high hardness (22.1 ± 0.2 GPa), high oxidation, and thermal shock resistance in extreme temperatures. Non-oxide ceramics have the disadvantage that their surface gets oxidized at elevated temperature, the important physical properties of oxide and non-oxide UHTCs are shown in Table 2.[1-7,31-32,44-46] Full densification of UHTCs faces major challenge due to strong covalent bonding, high-melting point and low diffusion rates. At low temperatures generally in case of borides, oxides layers covering boride particles surfaces get subjected to evaporation condensation mechanisms resulting in mass transfer without densification and at higher temperatures grain coarsening becomes predominant over densification.[3,4] As reported flexure strength of ZrB_2 and HfB_2 ceramics could be enhanced with addition of SiC or $MoSi_2$ as secondary phases from 300 to 500 MPa to 800-1000 MPa.[9] SiC and $MoSi_2$ are generally added as sintering aids to increase oxidation resistance by forming a silica glass protective layer on the surface when it is exposed to air at high temperature.[34] Desirable characteristics of ceramic powders for efficient compaction are shown in Figure 2. Physical properties of oxide and non-oxide UHTC's are given in Table 2. At high temperatures exceeding 2000°C, UHTCs retain their bending strength and hardness. Owing to strong covalent bonding, UHTC's exhibit high hardness (22.1 ± 0.2-23 ± 0.9 GPa). Mechanical and thermal properties of important diborides are shown in Table 3 and 4, respectively. Despite high melting points of UHTCs, they are unsuitable for many refractory applications because of their high susceptibility to oxidation at elevated temperatures.[47–51] HfB_2 oxidizes at 1100°C, while ZrB_2 oxidizes between 800°C and 1200°C[38] as per the following reactions in Equations 3 and 4:

$$HfB_2\,(s) + (5/2)\,O_2\,(g) = HfO_2\,(s) + B_2O_3\,(l) \quad (3)$$

$$ZrB_2 + 5/2O_2\,(g) \rightarrow ZrO_2 + B_2O_3\,(l) \quad (4)$$

Summarizing, it can be said that monolithic ceramics are susceptible to oxidation at high temperatures, therefore, addition of sintering additives is needed to increase the oxidation resistance at high temperatures and improve the properties of monolithic ceramic composites.[52-54]

4 | PROCESSING OF ZrB_2–SIC COMPOSITES VIA CONVENTIONAL, HOT PRESS, AND SPS PROCESSING TECHNIQUES WITH OR WITHOUT SINTERING ADDITIVES

Literature survey revealed that borides are generally combined with additives to increase oxidation resistance and strength; especially ZrB_2 composites with SiC addition processed via different sintering routes are best suited for use at ultra high temperatures because of their excellent properties of high hardness, high-melting point, and chemical stability at extreme temperature.[2,45] Compact powder samples are generally heated at high temperature resulting in atomic diffusion during sintering, reducing porosity, and densifying the sample. Generally, conventional sintering is the most suitable and economical processing technique, which allows sintering of different shapes. However, spark-plasma sintering (SPS) reduce processing time, lower sintering temperature and restrict grain growth with fast heating rate.[3-5] Before sintering, milling is generally preferred for diborides powders to improve densification, which homogenize the powders. It was observed that addition of sintering aids in ZrB_2

TABLE 2 Physical properties of oxide and nonoxide UHTC's[1-7,31-32,44-46]

Crystal	Structure	Lattice parameters (°A)			Density (g/cm^3)	Melting point (K)
		a	*b*	*c*		
Oxides						
Al_2O_3	Hexagonal	4.7850	4.7564	12.9894	3.99	2345
ZrO_2	Monoclinic	5.1454	5.2075	5.3107	5.68	2988
TiO_2	Tetragonal	4.5937	4.5937	2.9581	4.24	2116
SiO_2	Tetrahedral	4.9965	—	5.4546	2.64	1983
Non oxides						
HfB_2	Hexagonal	3.1420	3.1420	3.4800	11.1	3523
TiB_2	Hexagonal	3.0236	3.0236	3.2204	4.52	3503
ZrB_2	Hexagonal	3.1700	3.1690	3.5440	6.09	3273
Si_3N_4	Hexagonal	7.7727	7.75327	5.6565	3.44	2173
ZrN	Cubic	4.5675	—	—	7.09	3253
Ta_3N_5	Orthorombhic	3.8900	10.2200	10.2700	14.3	3363
$MoSi_2$	Tetragonal	3.2112	3.2061	7.8480	6.25	2303
$TiSi_2$	Orthorombhic	8.2671	4.8000	8.5505	4.08	1773
$NbSi_2$	Hexagonal	4.7980	—	6.5920	5.69	2203
$TaSi_2$	Hexagonal	4.7840	—	6.5680	9.09	2673
B_4C	Hexagonal	5.6330	5.6330	12.1640	2.52	3036
TaC	Cubic	4.4270	—	—	14.65	4153
SiC	Hexagonal	3.0860	3.0730	10.0530	3.21	3003
SiC	Polymorphs	—	—	—	3.21	2545

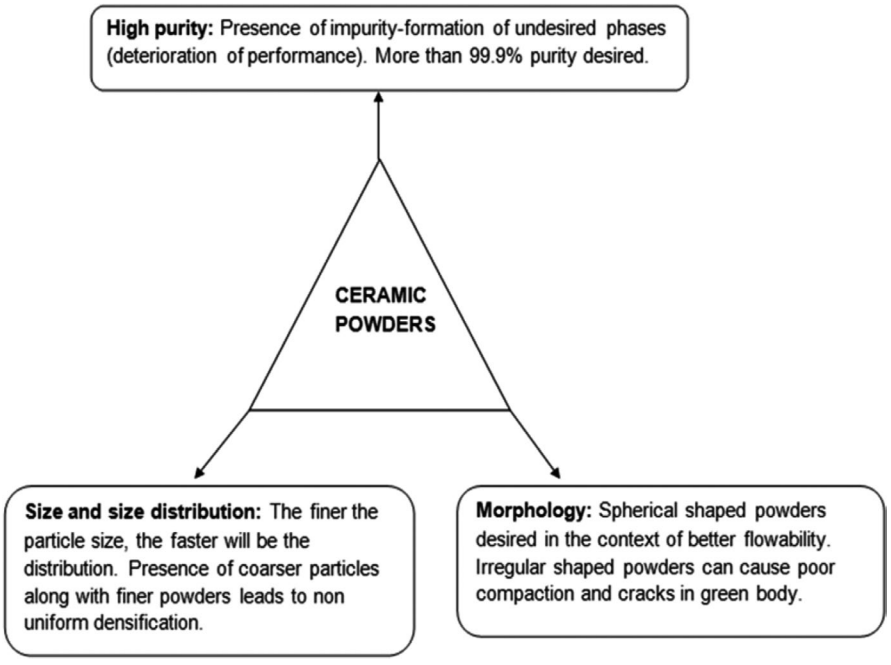

FIGURE 2 Desirable characteristics ceramic powders for efficient compaction

composites helped in removing oxygen impurities form diborides powders forming dense material during sintering.[46] Besides ZrB_2, additives like SiC can also be processed via non-conventional sintering reducing SiO_2 to SiO at 1500°C by vapor transport resulting 96% density at temperature between 1700°C and 1900°C with 70 MPa.[55] Properties obtained with different processing techniques used with or without additives for processing densified ZrB_2-based composites to have desired properties are shown in Table 4 and are sequentially discussed below.

TABLE 3 Mechanical properties of important diborides [2,4,9]

	Young modulus (GPa)	Flexural strength (MPa)	Hardness (GPa)
TiB_2	550	330 ± 40	33.0 ± 0.6
ZrB_2	500	305 ± 10	22.1 ± 0.2
HfB_2	500	350 ± 70	28.5 ± 0.5

4.1 | Influence of silicon carbide (SiC) addition on ZrB_2-based ceramic composites

Effects of addition of silicon carbide (SiC) on ZrB_2-based ceramic composites has been investigated by several researchers,[5,19,25,34,56-61] like Akina et al (2009)[5] synthesized ZrB_2–SiC composite via SPS route with sub-micron average particle size of ZrB_2 and α-SiC at different temperatures: 1800°C-1900°C for 300 seconds, at 2000°C-2100°C for 180 seconds and at higher temperature with no holding time. In general, SiC addition up to 60 wt% improved density of ZrB_2–SiC composite. Composites having 20-60 wt% SiC sintered at 2000°C-2100°C for 180 seconds reached a highest relative density of > 99%. Pores were visible in microstructure of composite with 80 wt% SiC addition. The porosity could have been resulted due to difficulty in sintering because of difference in thermal expansion coefficient of ZrB_2 and SiC. High temperature and pressure assisted sintering leads to microcracks due to thermal expansion anisotropy during cooling resulting in porosity and poor mechanical properties.[5] Abnormally grown texture of ZrB_2 and α-SiC grains caused the large pore formation at higher temperatures. Rezaie et al (2007)[33] examined the structure property of ZrB_2-30% vol SiC composites with different SiC particulate grain size (from ~1.2-3.1 μm) and ZrB_2 (~2.2-4.7 μm) at temperatures between 1850°C and 2050°C, along with times ranging from 45 to 180 minutes.[33] For the conditions established, high hardness of ≈22 GPa, fracture toughness of 5.5 $MPa.m^{1/2}$ and young's module between 501-516 GPa was reported, with maximum value obtained for ZrB_2 composite having SiC of 0.7 μm average particles size sintered at 1850°C for 45 minutes. Higher strength of ~1060 MPa at 1850°C with smaller grains and ~720 MPa at 2050°C with ~3.1 μm particle size of SiC grains is reported. The reason attributed to it is the larger SiC grains in the microstructure acted as the critical flaw causing the failure of the specimen, whereas smaller SiC grain sizes resulted in higher flexural strength for composite. Size and distribution of SiC influenced the toughness and strength of the composite by altering the amount of crack deflection.[33] Densified ZrB_2–SiC composites were prepared with 10-30 vol% SiC addition via hot press at 1900°C with 32 MPa pressure. Hardness of monolithic ZrB_2 increased from 23 ± 0.9 GPa to 24 ± 0.9 GPa with addition of 10 vol% SiC.[19] Strength of the composites were found to reach ~1 GPa and increased fracture toughness of 5.25 $MPa.m^{1/2}$ with 30 vol% SiC addition was obtained with increase in oxidation resistance of the composite.[34] Justin and Jankowiak[20] has developed ~98% dense ZrB_2–SiC composites hot pressed at 1700°C-1800°C for 2 hours at 27 MPa for leading edges of future hypersonic aircrafts. Addition of SiC increased oxidation resistance and restricted the diborides grains growth during sintering resulting in high hardness (20.9 ± 1.9 GPa) and fracture toughness (4.3 ± 0.2 $MPa.m^{1/2}$). Zhu et al (2006)[56] processed ZrB_2–SiC composites via hot press at 1900°C with 320 MPa. It was observed that SiC particle size controlled the strength of the composite. Smaller particle size SiC (0.45 μm) resulted in high densification (99.8%), finer grain size and high strength (909 MPa), whereas strength of 389 MPa could be achieved in ZrB_2–SiC composites with 10 μm sized SiC particles with presence of porosity. Larger particle size resulted in ineffective sintering accompanied with porosity which indicated that finer SiC particles are more effective pinning grain growth during sintering and restricts porosity. Asl and Kakroudi[57] compared monolithic ZrB_2 and ZrB_2-25 vol% SiC composite hot pressed at 1850°C for 60 minutes at 20 MPa and observed that grain growth was effectively stopped with SiC with increase in fracture toughness from 1.8-4.3 $MPa.m^{1/2}$. Increased density (99.7%) and high hardness of 22.71 GPa was found with 40 vol% SiC sintered via SPS at 1900°C for 15 minutes at 70 MPa. Indentation fracture was improved by toughening mechanisms via SiC addition.[58] Monolithic ZrB_2 reinforced with SiC sintered via SPS at 1650°C for 5 minutes at 40 MPa led to increase in density from 93.1% to 95% and hardness from 13.2 to 19.3 $MPa.m^{1/2}$.[60] Further their properties were evaluated with CNT addition discussed in later section. A preliminary investigation was done in processing of ZrB_2-15 vol% SiC ceramics via conventional and SPS routes at same sintering temperature with different holding times and compaction loads. ZrB_2 and SiC powders of particle sizes ~5 and ~1 μm respectively of purity > 95% were taken commercially. 5 vol% Ni (purity > 99%) of ~3 μm particle size was used as sintering additive. Powders were uniformly mixed by ball milling. The powders were compacted with 150 MPa uniaxial pressure and sintered at 1800°C for 2 hours in argon in a high resistance sintering furnace. ZrB_2–SiC composites were also processed via SPS at 1800°C for 5 minutes at 50 MPa. Density of 95% and >98.5 were obtained via conventional and SPS. Detailed results would be reported and discussed elsewhere. Increase in hardness and fracture toughness was achieved via SPS. Ni melt during sintering played a major role by acting as a binder for ZrB_2–SiC composites and affecting the properties of the composites.

TABLE 4 The summary of physical and mechanical properties of ZrB_2–SiC composites with or without additives

ZrB_2 µm	α-SiC µm	SiC vol%	Sintering Technique used	Additive	Holding Time (min)-	Pressure (MPa)	Temp (°C)	Relative Density	Strength (MPa)	Hardness (GPa)	Fracture toughness (MPa $m^{1/2}$)	References
2	—	~8	Pressureless	(PCS)	120	30	2000	96.7	374 ± 17	18.7 ± 0.6	3.1 ± 0.4	[44]
~2	0.45	10	Pressureless, (CIP)	Carbon + B_4C-4wt%	120	310	2000	~97	404 ± 62	15.3 ± 1.2	3.1 ± 0.1	[45]
~2	0.45	20	″	Carbon + B_4C-4 wt%	120	″	2000	>97	463 ± 53	18.8 ± 1.1	3.4 ± 0.1	[45]
~2	0.45	30	″	Carbon + B_4C-4 wt%	120	″	2000	>99	492 ± 49	22.4 ± 0.7	3.5 ± 0.3	[45]
2	1	60	SPS	—	3-5	20	2000-2100	~99	—	~26.8	3.5	[5]
2	1	50	″	—	3-5	20	1900-2100	~97	380	~25	4.1	[5]
2	0.7	30	Hot press	—	45	32	1850	97.2	~1070	20 ± 2	5.5 ± 0.3	[33]
2	0.7	″	″	—	45	32	1950	99	~1070	22 ± 2	5.2 ± 0.4	[33]
2	0.7	″	″	—	45	32	2050	>99.9	~850	23 ± 1	4.3 ± 0.2	[33]
2	0.7	″	″	—	90	32	2050	99	~850	22 ± 1	4.2 ± 0.1	[33]
2	0.7	″	″	—	180	32	2050	99.5	~800	22 ± 1	4.5 ± 0.2	[33]
—	—	—	Hot press	—	180	32	1900	103	565 ± 53,	23 ± 0.9	3.51 ± 0.33	[34]
—	—	10	″	—	180	32	1900	95	713 ± 48	24 ± 0.9	4.13 ± 0.30	[34]
—	—	20	″	—	180	32	1900	103	1003 ± 94	24 ± 2.8	4.41 ± 0.22	[34]
—	—	30	″	—	180	32	1900	104	1089 ± 152	24 ± 0.7	5.25 ± 0.46	[34]
—	—	—	Hot press	—	30	30	1900	87	~350	8.7±0.4	2.35±0.15	[77]
—	—	—	″	Si_3N_4-5 vol%	15	30	1700	98	~600	13.4±0.6	3.75±0.1	[77]
—	—	20	″	Si_3N_4-4 vol%	10	30	1870	98	~730	14.6±0.3	—	[77]
—	—	18.5	″	3.7Si_3N_4, 1Al_2O_3, 0.5Y_2O_3 vol%	10	30	1760	98	~710	14.2±0.6	4.55±0.1	[77]
~2.5	~0.5	20	Pressureless	Mo 4wt%	120	~200	2200	~99	~632	~16.3	4.6	[61]
~1.5-3	~1.5	10	Hot Press	B_4C 1 wt%	60	25	2000	99.8	393 ± 114	17.98 ± 0.9	3.76 ± 0.34	[62]
~1.5-3	~1.5	20	″	B_4C 1 wt%	60	25	2000	99.7	487 ± 68	22.13 ± 1.1	4.15 ± 0.83	[62]
~1.5-3	~1.5	30	″	B_4C 1 wt%	60	25	2000	97.5	425 ± 53	24.36 ± 0.6	4.44 ± 0.48	[62]
2-10	1 β SiC	5-25	Reactive hot pressed	B_4C, Ni	30	40	1400-1500	97-99.9	—	17.2 ± 2.9-22.3 ± 1.8	—	[64]

(Continues)

TABLE 4 (Continued)

ZrB_2 µm	α-SiC µm	SiC vol%	Sintering Technique used	Additive	Holding Time (min)-	Pressure (MPa)	Temp (°C)	Relative Density	Strength (MPa)	Hardness (GPa)	Fracture toughness (MPa $m^{1/2}$)	References
5 ~ 10	—	16	Hot press	Polycarbosilane (PCS)	60	20	2073	100	—	16.2	3.4	[89]
6	10	30	Hot Press	—	45	32	1900	97.4	389 ± 45	17.5±0.4	4.5±0.1	[56]
6	1.4	30	″	—	45	32	1900	98.9	805 ± 71	19.1 ± 1	4.3±0.3	[56]
6	0.7	30	″	—	45	32	1900	98.7	837 ± 116	19.3±0.6	4.2±0.2	[56]
6	0.45	30	″	—	45	32	1900	99.8	909 ± 136	20.7 ± 1	4.6±0.1	[56]
Zr, B4C, C, Si		25-30	Reactive hot press	Ni	30-60	40	1600	~98%	—	—	—	[142]
<2	<3	20	SPS	Graphene, 10 vol%	6	35	1800	100	—	—	—	[79]
~2	—	—	Hot press	—	60	20	1850	90	—	11.9	1.8	[57]
~2	~5	25	″	—	60	20	1850	94	—	13.5	4.3	[57]
~2	~5	25	″	Grapheme-5 wt%	60	20	1850	~99	—	~15.7	6.4	[57]
2	1	20	″	Graphite nano flakes −15 vol%	60	30	1900	99.7-100	387.18 ± 19.13-480.96 ± 25.17	10.8 ± 1.2-11.2 ± 0.5	4.3 ± 0.15-6.11 ± 0.25	[80]
1-2	—	—	SPS	—	15	70	1900	84.8	162 ± 31	16.64 ± 0.9	1.51 ± 0.02	[81]
1-2	—	—	SPS	GNP (2%-6%)	15	70	1900	84.5-96.9	204 ± 34-316 ± 85	13.5 ± 0.25-15.9 ± 0.84	2.1 ± 0.43-2.77 ± 0.06	[81]
2	0.5	20	Hot Press	—	60	30	1950	98.2	537 ± 45	23.07 ± 3.26	4.2 ± 0.31	[82]
2	0.5	20	Hot Press	Grapheme oxide—2 vol%	60	30	1950	98.9	698 ± 52	22.93 ± 1.83	6.07 ± 0.25	[82]
2	0.5	20	Hot Press	Grapheme oxide—5 vol%	60	30	1950	99.2	1055 ± 64	22.76 ± 2.07	7.32 ± 0.37	[82]
1.4	0.45	20	Hot press	—	60	30	1900	~96.9	582 ± 102	15.8 ± 0.3	4 ± 0.3	[143]
1.4	0.45	20	″	CNT, 2 wt%	60	30	1900	~96.0	616 ± 97	15.5 ± 0.9	4.6 ± 0.6	[143]
~2	—	—	Hot press	—	60	20	1850	90.1 ± 0.3	—	11.9 ± 0.4	1.8 ± 0.7	[86]
~2	~5	20	″	—	1 h, 20 MPa	20	1850	93.2 ± 0.4	—	13.1 ± 0.5	3.8 ± 0.4	[86]
~2	~5	20	″	CNT, 10 vol%	60	20	1850	93.9 ± 0.6	—	8.6 ± 0.3	5.1 ± 0.8	[86]
1-2	1	20	SPS	MWCNT 15 vol%	5-10	25-40	1600-1800	94.6-99.1	472-565	11.5-16	5.9-8.0	[87]

(Continues)

TABLE 4 (Continued)

ZrB_2 µm	α-SiC µm	SiC vol%	Sintering Technique used	Additive	Holding Time (min)-	Pressure (MPa)	Temp (°C)	Relative Density	Strength (MPa)	Hardness (GPa)	Fracture toughness (MPa $m^{1/2}$)	References
1-2	—	—	SPS	—	15	70	1900	84.8	162 ± 31	16.64 ± 0.90	1.51 ± 0.02	[58]
1-2	2	10	〃	—	15	70	1900	99.1	553 ± 07	19.38 ± 0.13	2.21 ± 0.25	[58]
1-2	2	40	〃	—	15	70	1900	99.7	410 ± 17	22.71 ± 0.19	2.31 ± 0.23	[58]
0.5-6	0.45	3	SPS	Si_3N_4-8 vol%; C fibres-45 vol%	1.5	60	1900	>96.7	200	—	—	[78]
10	40 nm	2.5-15 wt%	Pressureless sintering	C fibre 2.5-10 wt%	60		2100-2150	87-95	—	11-15	3-5.9	[65]
0.1-8	14; fiber	20	Hot Press	Si_3N_4, 5-10 vol%	10	40-50	1700	—	410 ± 20	—	5.7 ± 0.3	[70]
0.1-8	14; fiber	20	〃	$ZrSi_2$,5-10 vol%	10	40-50	1600	—	385 ± 13	—	6.2 ± 0.4	[70]
0.1-8	14; fiber	20	〃	$MoSi_2$, 5-10 vol%	10	40-50	1750	—	380 ± 20	—	4.8 ± 0.1	[70]
0.1-8	14; fiber	20	〃	$MoSi_2$, 5-10 vol%	10	40-50	1900	—	—	—	3.7 ± 0.3	[70]
8.17	0.60	20	Hot press	—	120	27	1800	~98	451 ± 90	20.9 ± 1.9	4.3 ± 0.2	[20]
8.17	0.60	20	Hot press	$TaSi_2$ −20 vol%	120	27	1800	~99	688 ± 79	18.1 ± 0.4	4.4 ± 0.2	[20]
0.5	1.5	10-30	Hot Press	PCS	60	28	1750	94-98	360-380	—	5.9-7.6	[90]
2	1	20	Hot Press	ZrO_2, 15 vol%	60	30	1850	98.6	1085 ± 118	18.4 ± 1.3	6.8 ± 0.6	[72]
10	—	—	SPS	B_4C-6 vol%	10	30	1850	>99	—	17.6 ± 2.1	8.9 ± 1.7	[66]
10	0.5	20	〃	B_4C-6 vol%	10	30	1850	〃	—	22.7 ± 1.1	11.3 ± 0.9	[66]
HfB_2-ZrB_2	0.5	20	〃	B_4C-6 vol%	10	30	1850	〃	—	25.3 ± 0.6	12.9 ± 0.6	[66]
HfB_2-ZrB_2	0.5	20	〃	B_4C-6 vol%, CNT-6 vol%,	10	30	1850	〃	—	27.2 ± 0.7	13.8 ± 0.4	[66]
<2	—	—	SPS	—	5	40	1650	93.1	—	13.2 ± 1.0	—	[60]
<2	<1	20	SPS	—	5	40	1650	95	—	19.3 ± 0.6	—	[60]
<2	—	—	〃	CNT-10	5	40	1650	95.9	—	18.6 ± 0.8	—	[60]
<2	<1	20	〃	CNT-10	5	40	1650	99.7	—	21.0 ± 1.7	—	[60]
~5	~1	15	Pressureless sintering	Ni −5 vol%	120	150	1800	95	390 ± 05	18 ± 0.9	3 ± 0.2	Present work
~5	~1	15	SPS	Ni −5 vol%	5	50	1800	>98.5	420 ± 20	21 ± 1.2	3.8 ± 0.2	Present work

4.2 | Influence of carbides and metallic binders with carbon as sintering additives on ZrB_2–SiC ceramic composite

Zhang et al (2010)[45] prepared ZrB_2-(10-30 vol%) SiC composites with B_4C and carbon via conventional sintering with 97% of densification. B_4C and carbon used as sintering additives removed surface oxides as oxide impurities from particles surfaces and inhibit densification. Excess carbon resulted in residual carbon formation at the ZrB_2/SiC grain boundaries, higher SiC content led to larger volume fraction of carbon at grain boundaries reducing composite strength. It is reported that hot pressing result in maximum densification even without addition of sintering aids but sintering aids as borides, silicides, metals (eg, Ni), or C were used to lower sintering temperature and processing time. High densification in diborides can be achieved at 1900°C and 30-50 MPa via hot press.[10] ZrB_2–SiC composite with 4 wt% Mo as sintering additive was prepared via conventional sintering at 2200°C for 2 hours A cold isostatic pressure of ~200 MPa for 2 minutes was used to prepare powder compacts. Relative density of ~99% with 560 MPa strength was achieved for the processed composite.[61] Patel et al[62] processed hot pressed ZrB_2-(10-30 vol%) SiC composites with B_4C (1 wt%) as sintering additive. With higher SiC content, density decreased from 99.8% for ZrB_2-(10 vol%) SiC to 97.5% for ZrB_2-(30 vol%) SiC, whereas there was increase in hardness and fracture toughness with increasing SiC content. It was found that exposure of composites at 1000°C for 5 hours result in following reaction as per Equations 5-8:

$$ZrB_2 + 5O_2 = 2ZrO_2 + 2B_2O_3\,(l) \tag{5}$$

$$2SiC + 3O_2 = 2SiO_2 + 2CO \tag{6}$$

B_4C used as sintering aid undergo following conversion:

$$2B_4C + 7O_2 = 4B_2O_3\,(l) + 2CO \tag{7}$$

$$B_2O_3\,(l) = B_2O_3\,(g) \tag{8}$$

B_4C (sintering additive) gets oxidized and glassy B_2O_3 (l) evaporates at sintering temperature, between 1200 and 1600°C. ZrB_2–ZrC_x–SiC_p composites were processed using Zr–B_4C powder mixtures with SiC particulates via reactive hot press at low temperatures 1400°C-1500°C for 30 minutes and 40 MPa pressure. Higher density and high hardness from ~ 17-22 GPa was found with use of fine reactant powders.[63,64] Nasiri et al[65] processed ZrB_2–SiC–C_{sf} via pressureless sintering at 2100°C-2150°C with addition of nano-SiC and short carbon fibers. Optimal percentage of 2.5 wt% carbon fiber and 10 wt% SiC nanoparticles resulted in increase in hardness and fracture toughness from 2100°C to 2150°C. Nisar et al[66] processed densified ZrB_2–B_4C and ZrB_2–SiC–B_4C composites sintered via SPS at 1850°C for 10 minutes at 30 MPa and found increase in toughness (8.9 to 11.3 MPa.$m^{1/2}$) of the composite due to toughening effect of B_4C and SiC.

4.3 | Influence of silicide, oxides, and borides as sintering additive on ZrB_2–SiC ceramic composite

Chamberlain et al[34] prepared pure ZrB_2-based composites with 10, 20, or 30 vol% of SiC or $MoSi_2$ via hot press at 1900°C with 32 MPa pressure. Hardness and fracture toughness were found higher with 10 vol% $MoSi_2$. Theoretical density from 101%-103% was achieved with increasing 30 vol% $MoSi_2$ addition. It was observed that $MoSi_2$ addition has decreased the oxidation resistance of the composites as compared to monolithic ZrB_2. The highest hardness and fracture toughness values (24 GPa and 5.25 MPa.$m^{1/2}$, respectively) were obtained for compositions containing SiC; increase in toughness may be due by crack bridging by SiC particulates. On the contrary, $MoSi_2$ provided the highest young module and flexure strength values (523 GPa and 1151 MPa, respectively).[34] Francois and Jankowiak[20] have developed ZrB_2–SiC and ZrB_2–SiC–$TaSi_2$ composites for leading edges of future hypersonic aircrafts. Addition of SiC increased oxidation resistance and restricted the diborides grains growth. Addition of $TaSi_2$ lowered the oxidation rate by reducing the concentration of oxygen vacancies and decreasing oxygen transport through the growing oxide scale. Composites were hot pressed at 1700°C-1800°C for 2 hours at 27 MPa. Addition of $TaSi_2$ resulted in high strength (688 ± 79 MPa) and fracture toughness (4.4 ± 0.2 MPa.$m^{1/2}$) n ZrB_2–SiC composite. Bellosi et al[67] processed ZrB_2–15 vol% $MoSi_2$ composite via SPS and hot press. SPS resulted in dense material in comparison to hot press processed composites. High temperature strength was found high in SPS-sintered samples with lower flexural strength in composites processed by hot press. Addition of $MoSi_2$ led to the silica-based layer formation resulting in effective oxidation control. Zamora et al[68,69] explored the densification of ZrB_2 by SPS without additives. Densified nanoscale ZrB_2 was prepared with SPS at 1625°C with 75 MPa and 100°C/min heating rate. Densified nanoscale ZrB_2 can be obtained at 1450°C in presence of B_2O_3, but remain unsuitable for high temperature applications. ZrB_2–SiC composite properties depend on various factors like SiC content, grain size, and temperature range. SiC chopped fibers addition up to 20 vol% has led to improvement in fracture toughness of ZrB_2 ceramics processed via hot press at 1600°C-1900°C. Higher fracture was observed with $ZrSi_2$ addition as sintering aid to ZrB_2–20 SiC fiber in comparison to Si_3N_4 and $MoSi_2$ addition as sintering aid.[70] ZrB_2–SiC ceramics with addition of ZrO_2

fibers hot pressed at 1850°C resulted in increased fracture toughness by enhancing fiber pull out, bridging and branching of cracks. SiC chopped fibers addition up to 20 vol% has led to improvement in fracture toughness of ZrB_2 ceramics processed via hot press at 1600°C-1900°C. Higher fracture toughness was observed with $ZrSi_2$ addition as sintering aid to ZrB_2–20SiC fiber in comparison to Si_3N_4 and $MoSi_2$ addition as sintering aid.[70] Generally, below 800°C, ZrB_2–SiC composite remain stable whereas fast oxidation of ZrB_2 and slow oxidation of SiC occur between 800°C and 1200°C forming ZrO_2 and SiO_2. Hardness and fracture toughness increased with SiC content from 10-30 vol%. Between 700°C and 1200°C, the oxide structure consisted of unaffected ZrB_2–SiC in the substrate, and a subscale of ZrO_2 containing unoxidized SiC and a B_2O_3-rich outer layer as per the following reactions in Equations 9 and 10.[70,71]

$$ZrB_2 + 5O_2 = 2ZrO_2 + 2B_2O_3\,(l) \tag{9}$$

$$SiC + 3/2O_2 = SiO_2 + 2CO \tag{10}$$

ZrB_2–SiC ceramics with addition of ZrO_2 fibers hot pressed at 1850°C resulted in increased fracture toughness by enhancing fiber pull out, bridging, and branching of cracks.[72] It was observed by Chakraborty et al[73] that TiB_2 addition in ZrB_2 resulted in improved mechanical and wear resistance. Hot pressed at 2200°C for 2 hours in argon TiB_2 entered completely into ZrB_2 structure during sintering forming solid solution with it. In comparison of monolithic ZrB_2 addition of TiB_2 up to 30 wt% showed high hardness and fracture toughness of 22.34 GPa and 3.01 $MPa.m^{1/2}$, respectively. Fully dense HfB_2–ZrB_2–SiC composites were processed with addition of B_4C and CNT via spark plasma sintering at 1850°C. Though the mechanical properties were enhanced with CNT by suppressing crack formation as discussed in later section, also the augmentation in the mechanical properties established the synergy between solid solution formation (with the equimolar composition of HfB_2/ZrB_2) and reinforcements led to improvement in properties of the composites.[74,66,75,60] It was reported that HfB_2-ZrB_2 system led to full densification and increase in fracture toughness (5.2 to 10.2 $MPa.m^{1/2}$). Due to their nature of forming solid solution during sintering with SiC and CNT addition.[76]

4.4 | Influence of carbides and nitrides with carbon as sintering additives on ZrB_2–SiC ceramic composite

Several researchers had investigated the effect of carbides and nitrides with or without carbon on physical and mechanical properties of ZrB_2–SiC composite. Zhang et al[45] explored the effect of carbon addition in ZrB_2–SiC composites and found that higher content of carbon additions (10 wt% based on SiC) resulted excess carbon at grain boundaries. It led to decrease in flexural strength of the composite, whereas increasing SiC content (10-30 vol%) with 5 wt% carbon addition resulted in increase in hardness, flexural strength, and toughness of the composite as shown in Table 4. Monteverde et al (2002)[77] found that sinterability of ZrB_2 was highly improved with Si_3N_4 addition as sintering aid in comparison to additive free ZrB_2. Full densification of ZrB_2 composite was achieved at 1700°C by hot press with 20 vol% SiC and 5 vol% Si_3N_4 addition. Si_3N_4 resulted in liquid phase formation at onset temperature, which increased the densification rate and powder compact shrinkage. Presence of SiC particles exhibited a clustered distribution with secondary phases. It was found that presence of SiC particles in ZrB_2 composites effectively improved the properties compared to monolithic ZrB_2. Bellosi et al[67] processed ZrB_2-based composite via SPS and hot press with ZrC and ZrC-Si_3N_4 addition in ZrB_2–SiC composite. SPS resulted in dense material in comparison to hot press processed composites. High temperature strength was found high in SPS sintered samples with lower flexural strength in composites processed by hot press. Addition of 45 vol% carbon fibers (C_f) in ZrB_2–SiC–Si_3N_4 ceramics sintered via SPS at 1800°C-2300°C with different holding times resulted in density of 96.7% sintered at 1900°C. Increase in temperature from 1850°C to 1900°C did not affect the densification. Extreme damage of carbon fibers was observed with use of ~3000°C/min heating rate, therefore, precise temperature control is required to achieve high density while preserving the fibers structural and morphological integrity. Due to high heating rate and difficulty in precise control of temperature above 1900°C, carbon fiber degradation was noticed in micrographs which resulted in brittle behavior of composite.[78]

4.5 | Influence of graphene as sintering additive on ZrB_2–SiC ceramic composite

Density and mechanical properties of ZrB_2–SiC ceramics can be improved by adding graphene nano plates as additive. Homogeneous diffusion of carbon led to smooth interface formation between SiC and graphene nano plate at 1800°C in SPS and due to nonreactive role of grapheme during sintering, no ZrC or B_4C were formed.[79] Addition of 5 wt% grapheme platelets increased the density (>99%) of ZrB_2–SiC ceramic hot pressed at 1850°C with high hardness and indentation fracture toughness in comparison to monolithic ZrB_2 or ZrB_2–SiC ceramics. Graphene promoted crack deflection and bridging resulting in high toughening of composite.[57] Similar results of anisotropy in fracture toughness and flexural strength with 15 vol% graphite flakes in ZrB_2–SiC composite hot pressed at 1900°C were reported by Zhou

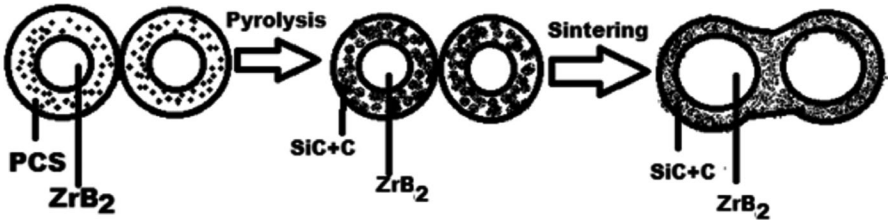

FIGURE 3 Microstructure development schematic for ZrB_2 and with PCS[89]

et al.[80] Addition of 2-6 vol% grapheme nanoplates (GNPs) to ZrB_2 ceramic sintered via SPS at 1900°C increased the density of ZrB_2 (84.8%) to ZrB_2-GNPs (96.9%) with decrease in hardness and increase in fracture toughness and flexural strength.[81] Graphite flakes addition to ZrB_2–SiC ceramics hot pressed at 1900°C increased the fracture toughness with slightly decrease in hardness and flexural strength.[82] In general, uniform dispersion and avoiding agglomeration has always been a challenge with adding graphene or CNT (discussed in later section) as reinforcement in the ceramic matrix. Therefore, several dispersion techniques like conventional ball milling, in situ thermal reduction of graphene oxide have been used to overcome these problems.[82,83] Due to limitation of reaction between ceramic precursors and graphene sheets at high temperature pyrolysis, addition of graphene in ZrC–SiC composites was incorporated via slurry infiltration followed by SPS by Cheng et al[84] accomplishing high density (97.6%), fracture toughness (4.3 $MPam^{1/2}$), and strength (220 MPa).

4.6 | Influence of CNTs as sintering additive on ZrB_2–SiC ceramic composite

Toughness of ZrB_2–SiC ceramics increased with no significant effect on hardness or strength of the composite on 2 wt% CNT addition sintered via hot press at 1900°C. Crack propagation with deflection was found less in ceramics without carbon nanotube (CNT), whereas cracks were found to be deflected and bridged by CNTs addition.[85,79] Similar conclusion were drawn by Shahedi Asl et al[86] and Lin et al,[87] respectively, with addition of 10 vol% CNT to ZrB_2–SiC ceramics hot pressed at 1850°C and with 15 vol% CNT addition sintered at 1750°C via SPS. Similar result was reported by Yadhukulakrishnan et al.[58] Density > 99% was achieved with addition of 4%-6% CNT addition and indentation fracture toughness was improved due to toughening mechanism. Addition of B_4C and CNT in HfB_2–ZrB_2–SiC composites has not only beneficial for densification, but also increased the indentation fracture toughness three times (13.8 $MPa.m^{1/2}$) than of monolithic HfB_2/ZrB_2 (3-4 $MPa.m^{1/2}$) suppressing crack formation by deflecting and bridging them.[66] Similar conclusions were drawn by Nisar et al[75] in their work where addition of CNT to ZrB_2–SiC composite resulted in dense, crack free microstructure. CNT embedded in the matrix retaining its structure during sintering at 1850°C. Addition of SiC/CNT/B_4C in ZrB_2 help in removal of surface oxide from the ceramic during sintering, which inhibited the sintering process.[66,75] Nisar et al[60] in their work enhanced the structural stability and oxidation resistance at extreme thermal temperatures (>2400°C) by reinforcing ZrB_2 with SiC and CNT. Synergistic addition of SiC and CNT in ZrB_2 resulted in increased thermal stability, decreased oxidation rate, and suppressed crack formation of the composite as cracks were found to be deflected and bridged by CNT addition.

4.7 | Influence of precursor and dispersants on ZrB_2–SiC ceramic composite

Pre ceramic polymers have been developed as precursors for composites, coatings, and fibers. Fine grain size can be obtained at lower processing temperature for preceramic polymer-derived ceramics.[44,88–93] Polycarbosilane polymer is used to obtain ceramic powder by pyrolysis with an advantage of having fine grain size at lower processing temperatures.[39,94–97] Dense ZrB_2–SiC composites can be synthesized via pressureless sintering with increase in relative density from 62.5% to 96.7% by coating the starting ZrB_2 powder with polycarbosilane, which gets converted to C and SiC by pyrolysis.[44] A density > 99% was achieved for ZrB_2-27 vol% SiC composites prepared by in situ reactive hot pressing at 1890°C for 10 minutes from stoichiometric ZrH_2, B_4C, and Si of submicron particle size as precursors. Powder reactions occurred at 1150°C to 1400°C temperature with reactive hot pressing in between 1600°C and 1900°C. Excess B_4C provided sufficient B to react with all Zr to produce ZrB_2.[88] Hot press, increased the relative density from 78% (without PCS addition) to 100% (with 16% SiC derived from PCS addition) of ZrB_2–SiC–C ultra high temperature ceramics (UHTCs) sintered at 2073 K for 60 minutes at 20 MPa in an argon atmosphere.[89] Microstructure development schematic is proposed based on the microstructure for samples with PCS are shown in Figure 3. ZrB_2 without PCS imparted grain distortion, rearrangement, and surface diffusion forming a network structure.[89] Densified ZrB_2 ceramics were developed with addition of SiC whiskers (SiCw) and PCS (polycarbosilane). ZrB_2–SiC_w–PCS slurry hot pressed at 1750°C where SiC_w played the role of deflecting and bridging the cracks resulting in higher fracture toughness (7.57 $MPa.m^{1/2}$) than of

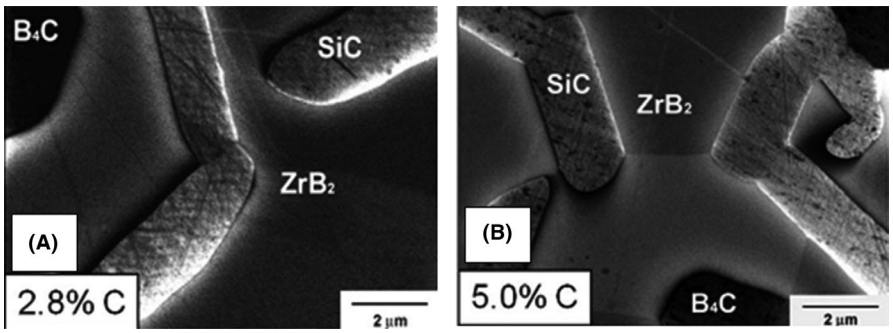

FIGURE 4 Microstructures of the ZrB_2–SiC containing 30% SiC in volume with (A) 2.8 wt% carbon, and (B) 10 wt% carbon[45]

monolithic ZrB_2 or ZrB_2–SiC_p (4.0-4.4 MPa.$m^{1/2}$). PCS being volatile may cause porosity so 9.1 wt% PCS was optimized to process dense ZrB_2–SiC_w ceramics.[87] Porous ceramics from polysiloxanes precursors offered simple processing method, low processing cost, and porosity control. Si(O)C-based ceramics can be synthesized from polysiloxane precursors via different processing strategies like replica, sacrificial template, direct foaming, and the reaction technique.[98] Polymer derived ceramics (PDCs) based on Si–O–C (silicon oxy carbide, SiOC) have become important because of low processing temperature (1000°C-1200°C), excellent thermal shock resistance, inherent chemical durability, mechanical strength, despite the amorphous phase.[99–109] Amorphous Si–Al–O–C ceramics can also be prepared by pyrolysis of poly (methylsilsesquioxane) precursors after treating them by the sol-gel-technique with an Al-containing alkoxide compound, namely alumatrane. These ceramics are more stable at high temperature in comparison to Al-free SiOC composites.[108,110]

Dispersants are generally used for uniform dispersion, that is, mixing of two different powders, further they either evaporate or get dissolve in the solution. Zhang et al (2011)[111] fabricated nano sized ZrB_2 composites using ZrB_2 nano powder (60 nm, purity > 95%), and SiC nano powder (40-50 nm) as raw materials and studied their dispersion behavior in ethanol solutions with different dispersants (Solspers 20000, NK-1 (micro/nano powder dispersant) and PEI polyethylene imine (10000). The suspension containing the Solspers 20000 was completely clear after 1 day sedimentation, indicating unsuitable for dispersing ZrB_2 and SiC nano powder. PEI content 0.7 and 2.5 wt% below pH 10 is preferred for ZrB_2 and SiC nano powders, respectively, for dispersion and co-dispersion in ethanol solution. PEI was also found suitable for of ZrB_2 powder confirmed by Lee et al (2007).[112] Lee et al (2007)[112] studied the dispersion behavior of ZrB_2 powder in aqueous solutions with polyethylenimine (PEI) dispersant and found it efficient for aqueous ZrB_2 slurries. For preparing highly concentrated aqueous ZrB_2 slurries, ZrB_2 powder (particle size: 2.12 µm) with varying PEI content (600-700 mol wt%) was studied. Result showed isoelectric point (IEP) of ZrB_2 moved from pH 5.8 to 6.2 after milling for 72 hours and moved to pH 11 with PEI regardless of dispersant molecular weight. PEI with MW 10 000 was concluded as most suitable dispersant for ZrB_2 among the tested ones. Dispersion of ZrB_2 suspensions in aqueous solution with Lopon 885, an ammonium polyacrylate solution as dispersant was studied by Lu et al (2009)[113] in aqueous tape casting of ZrB_2 powder with B_4U as sintering additives. Well dispersed ZrB_2 suspensions was obtained in alkaline pH range with 0.4 wt% dispersant. Huang et al (2007)[114] investigated the dispersion of ZrB_2 with ionic ammonium polyacrylate or a nonionic alkoxylated polyether dispersants (Darvan 821A and WA-1, respectively) and zeta potential was measured as pH function. It was observed that both dispersants increased the relative zeta potential (−50 mV to −110 mV) and exhibited consistent extrusion behavior to produce sintered, complex 3-D components from ZrB_2. So, it can be summarized that different dispersants plays an important role in effective mixing of ZrB_2, SiC powders.

5 | MICROSTRUCTURAL FEATURES OF ZrB_2–SIC CERAMIC COMPOSITES PROCESSED WITH OR WITHOUT SINTERING ADDITIVES

Micrographs obtained of the sintered ZrB_2–SiC ceramic composites play an important role in achieving desired physical and mechanical properties. Zhang et al[45] studied the influence of the amount of carbon on the resistance of pressurelessly sintered ZrB_2–SiC composite. Following the criterion of Griffith, relatively small grains resulted in ceramic materials with higher strength.[45] Resistance values lower than 400 MPa were reported for ZrB_2–SiC containing 30% of SiC with average particle size of, approximately, 6 µm; on the contrary, resistance values above 900 MPa were reported with SiC particle sizes of, approximately, 1 µm, or smaller.[45] These researchers showed that the highest flexure strength values were obtained to 5 wt% of carbon, whereas flexure strength decreased for 10 wt% of carbon, under 20% and 30% of SiC—in volume due to the high amount of SiC (20% and 30%), which resulted in a high volumetric fraction of excess carbon deposited in grain contours. Figure 4 feature ZrB_2–SiC microstructures containing 30% of SiC in volume, with carbon addition

of (a) 2.8 wt%, (b) 5 wt%, (c) 7.3 wt%, and (d) 10 wt%.[45] Under room temperature, factors such as fine mean grain size and defect density influence on flexure strength of ZrB_2–SiC. Like other fragile materials, the strength of ZrB_2–SiC is influenced by the largest flaws present in its microstructure. In addition of improving the mechanical properties of ZrB_2–SiC, smaller SiC particles reduce the tendency of microcracking and the nucleation of larger critical flaws.[2] In fact, for ZrB_2–SiC, resistance increased with decreased grain size of the SiC.[2] The microstructure of the ZrB_2–SiC can also be controlled by conducting a high (fast) heating rate next to reduced processing times.[5] Akin et al[5] prepared spark plasma sintered ZrB_2 (average particle size of 2 μm) composite with α-SiC (average particle size of 1 μm), under different temperatures and sintering times (Figure 5). Under 1900°C and 2100°C, the microstructure consisted of equiaxed ZrB_2 grains of 2-5 μm in size and α-SiC grains of 2-4 μm in size. Elongated grains of α-SiC formed under 2120°C and 2200°C, a laminar texture, similar to an eutectic texture, and irregular texture was obtained without holding time. For amounts of SiC above 50% in bulk, there was pore formation in the microstructure of ZrB_2–SiC. Consequently, hardness, module of longitudinal elasticity, fracture tenacity, and flexure strength also decreased. Monteverde et al[12] hot pressed ZrB_2–15SiC and ZrB_2–15SiC–10HfB_2 composites. Microstructure revealed formation of discrete shell around ZrB_2 enriched of Mo or Hf/Mo, core and residual glass. SiC particles in the ZrB_2 matrix, or in agglomerates include silica-based glassy residues (Figure 6). Addition of SiC can provide microstructures that improve the mechanical properties of ZrB_2–SiC composites—like hardness and fracture toughness—when compared to the monolithic ZrB_2 by enhancing their density.[77] Monteverde et al[77] processed monolithic ZrB_2 and ZrB_2 composite with Si_3N_4 or SiC—Si_3N_4 hot pressed at 1900°C as explained in above section. Grain growth was observed in monolithic ZrB_2 with slow densification due to surface oxide formation. Si_3N_4 added composite showed regular microstructure with flat grain boundaries (Figure 7) with highest fracture toughness (4.55 $MPa.m^{1/2}$) with Al_2O_3 and Y_2O_3 addition. Among the types of processing developed to obtain ZrB_2–SiC, the "hot-pressing" is what provides the best mechanical properties.[77] However, differences in the values of strength and toughness can be, among other factors, attributed to the different techniques of obtaining ZrB_2–SiC, so processes such as high-temperature self-sustaining sintering (SHS) or spark plasma sintering (SPS) can influence the mechanical properties of ZrB_2–SiC, with hardness, longitudinal elasticity module, fracture toughness, flexure strength, and bending strength, due to change in its microstructure.[88] ZrB_2 has a terrible sinterability, characteristic of this, intrinsic to this material. Because of this, it is very difficult, technically, to get a full density of pure ZrB_2 without adding additives such as SiC.[61] Bellosi et al[67] manufactured specimens under three different compositions as mentioned in above section found regular ZrB_2 grains and ductile $MoSi_2$ phase with irregular shape in ZrB_2–$MoSi_2$ composite. SPS-processed composite resulted in finer microstructure and restricted grain coarsening in comparison to hot press processed composite. Further, ZrC or ZrC–Si_3N_4 added composite revealed fine and uniform grains. However, the chemical and mechanical properties of ZrB_2-based ceramic composite can be improved by reducing grain size and minimizing impurities present in the microstructure.[56] Zhu et al[56] produced ZrB_2–SiC specimens varying the average particle size of SiC (≈10, 1.4, 0.7 and 0.45 μm), Figure 8 shows the microstructures obtained.[56] The highest young's module value was reported for the material formed with SiC with an average particle size of 0.45 μm, reaching 524 GPa and fracture toughness ranged from ≈4.2 to ≈4.6 $MPa.m^{1/2}$ (values greater than that reported for ZrB_2: ≈3.5 $MPa.m^{1/2}$). As the working temperature has a significant influence on microstructure development during sintering and on resulting mechanical properties of ZrB_2, a significant decrease in hardness, fracture toughness, and flexural strength is reported, above 1200°C-1400°C, in addition to oxidation and corrosion resistance.[115] Gupta el al.[115] found uniform distribution of SiC (dark phase) in ZrB_2 (bright phase) in the microstructure of ZrB_2–SiC composite processed via spark plasma sintering (SPS), under 1400°C during 6 minutes holding and 1600°C

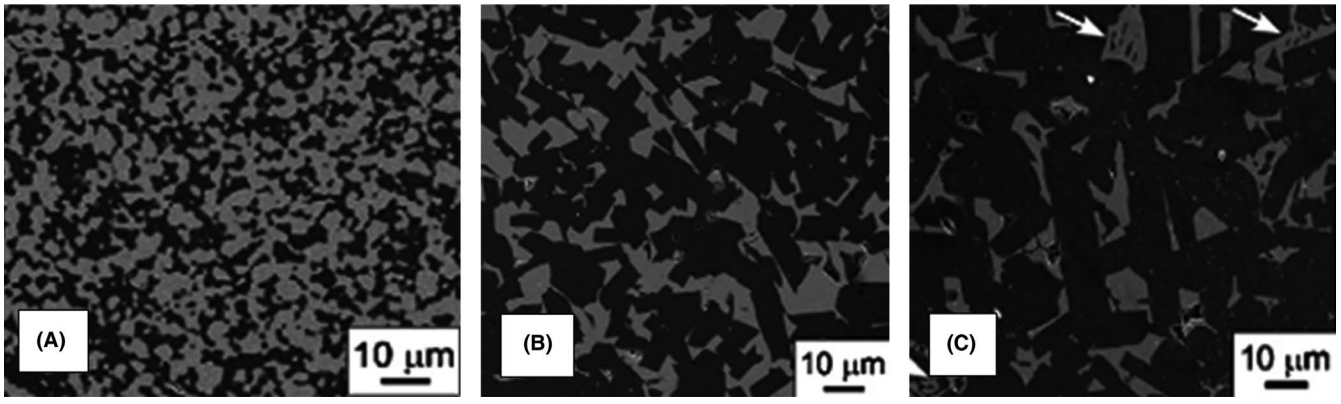

FIGURE 5 SEM images of ZrB_2–SiC composites containing 40 mass% SiC sintered at (A) 1900°C for 300 s, (B) 2120°C, and (C) 2200°C[5]

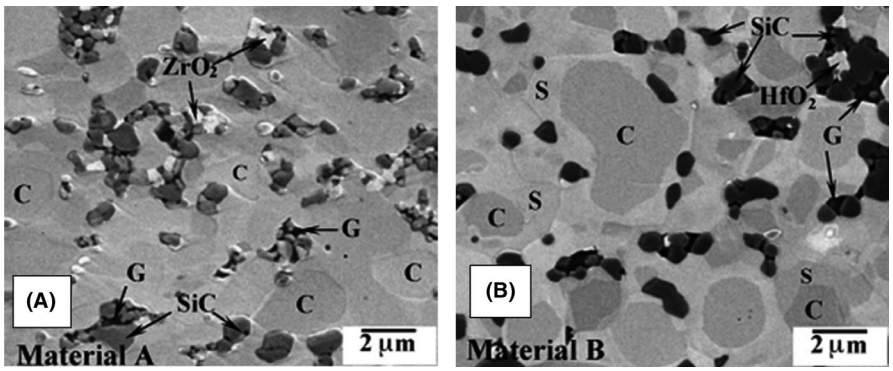

FIGURE 6 Microstructures of the materials (A) ZrB_2–15SiC and (B) ZrB_2–15SiC–10HfB_2 showing shell (S), core (C), and residual glass (G)[12]

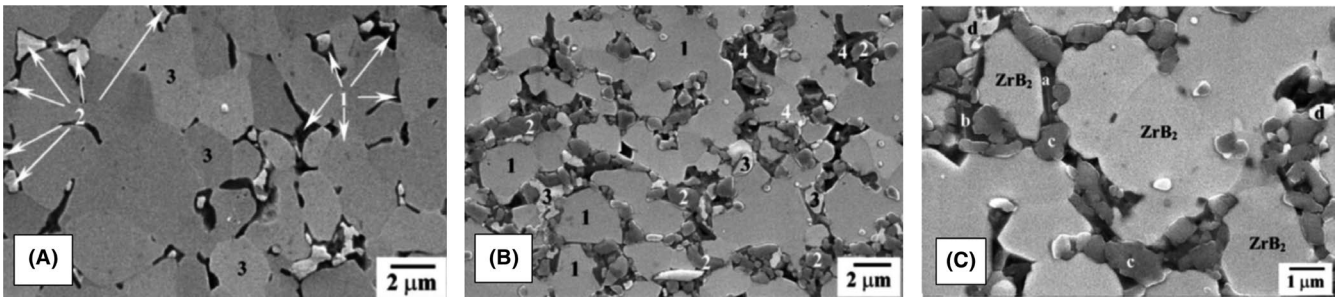

FIGURE 7 Microstructures of materials (A) ZrB_2–5Si_3N_4, (B) ZrB_2–20SiC-/4Si_3N_4, and (C) ZrB_2-/18.5SiC-/3.7Si_3N_4/-Al_2O_3-/0.5Y_2O_3—in sequence[77]

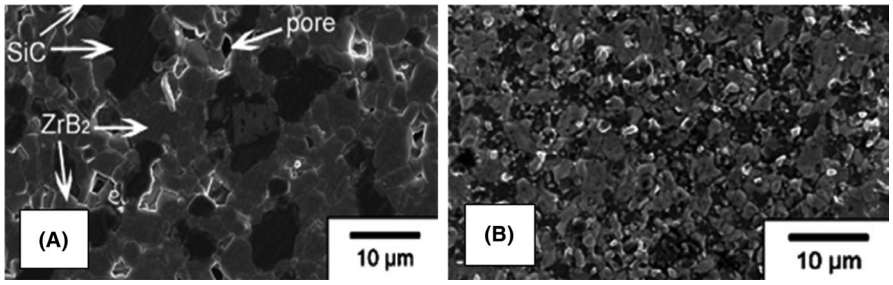

FIGURE 8 Microstructures for the different granulations of SiC: (A) 10 μm, (B) 0.45 μm[56]

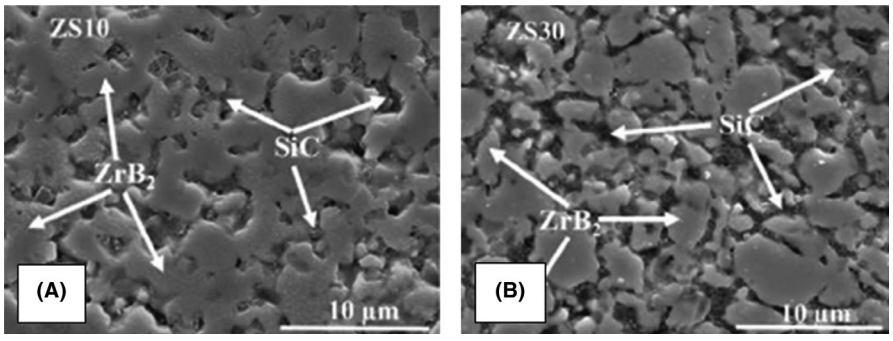

FIGURE 9 Microstructures of ZrB_2–SiC specimens obtained for the different volumetric percentages of SiC: (A) 10%, (B) 30%[115]

during 2 minutes holding, under a pressure of 55 MPa and a heating rate of 200°C/min, in an argon atmosphere and reported increase in hardness and fracture toughness values with increased amount of SiC. Figure 9 presents images of the microstructures of ZrB_2–SiC specimens obtained for the different volumetric percentages of SiC: (a) 10%, (b) 20%, and (c) 30%. Hardness increased from 18 to 23 GPa and fracture toughness increased from 4.2 to 5.3 MPa.$m^{1/2}$ when the amount of SiC increased from 10% to 30%, in volume.[115] Adopting the same sintering process and conditions used by Gupta et al[115]—spark plasma sintering (SPS), Sharma et al[116] further studied high-temperature erosion behavior. However, the improvement in mechanical properties is due to the fact that SiC addition promoted a better sintering of ZrB_2—which

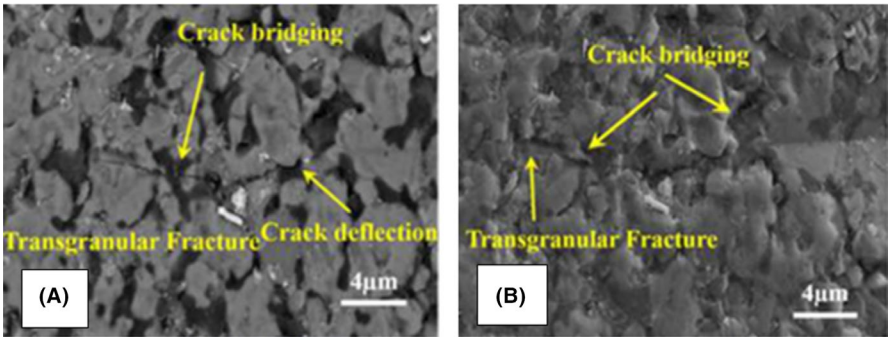

FIGURE 10 Occurrence of transgranular fracture, crack deflection and crack brindging for specimens containing (A) 10% SiC and (B) 30% SiC[116] [Color figure can be viewed at wileyonlinelibrary.com]

should be performed at high temperatures due to covalent connections[116]—decreasing the porosity of the material as visible in microstructure. Besides, Sharma et al[116], through propagation analysis of indentation crack, reported crack deflection or bridging by SiC particles. Additionally, Sharmaetal[116] observed transgranular fracture along the grains of ZrB_2, while crack bridging or crack deflection lead to an increase in fracture toughness. Consequently, a high amount of SiC leads to a large extent of "crack bridging" or "crack deflection," so as to maximize fracture toughness.[116] Figure 10 shows the microstructure with occurrence of transgranular fracture, crack deflection, and crack bridging for specimens containing 10% and 30% of SiC. However, depending on the application temperature for which ZrB_2 is directed, even these metallurgical procedures may not be sufficient to check the necessary characteristics to ZrB_2. With this, it is necessary, too, the addition of SiC, as a second phase, to enhance the mechanical properties of monolithic ZrB_2 as it has strengthening/toughening capabilities.[117] In the same line of analysis, Zhang et al[117] reported that SiC particles, located in the boundary of the ZrB_2, enhanced the binding between the ZrB_2 particles but higher SiC content did not affect significantly the density of ZrB_2–SiC composites processed via SPS at 1375°C and 25 MPa for 5 minutes. Figure 11 shows images of polished surfaces of ZrB_2–SiC specimens for 15% and 30% SiC resulting in higher grain size from 5 to 10 μm of SiC particle with increasing SiC content with no grain growth in ZrB_2 grains. Hardness values of 10.5 and 11.1 GPa were obtained, and flexural strength values of 335.5 and 391.6 MPa, for volumetric percentages of 15% and 30% SiC, respectively.[117] In addition to SiC, Zhang and Kurokawa[118] included B_4C in ZrB_2, in the amount of 1 wt% with 0-30 wt% SiC. The compacts were pressurelessly sintered for 3 hours at 2523 K. Oxidation behavior at 1273 and 1473 K revealed microstructure featuring two oxide layer of continuous glassy layer and ZrO_2 layer having unoxidized SiC at 1273 K and oxide layer of ZrO_2 and SiO_2 with unreacted SiC was found at 1473 K. For these conditions, it was observed that the relative density was between 96.5% and 98.2%. For ZrB_2–SiC composite processed via hot press with 30% SiC in volume, Neuman et al[119] observed micro cracks in microstructure due to large SiC clusters (Figure 12). Strength, longitudinal elasticity module, and fracture toughness were measured under different temperatures, ranging from room temperature up to 1600°C. For the three mechanical properties considered, a decrease was reported with increase in temperature.[119] Under room temperature, fracture toughness can be affected by the presence of stress-induced micro-cracks, so as to decrease it. Besides, spontaneous microcracks reduced the fracture toughness by two mechanisms: reducing the initial modulus and linking with the main crack during fracture. On the contrary, to spontaneous microcracking, stress-induced microcracking improve the fracture toughness by shielding the crack tip and dissipating the fracture energy during crack propagation. However, pre-existing microcracks, such as the spontaneous microcracks formed by thermal expansion mismatch, do not contribute to crack tip shielding.[119] Wang et al[120] reported that ZrB_2 composite containing "nano-SiC whiskers," "nano-SiC whiskers + AlN" or "nano-SiC whiskers + Si_3N_4" increased the bending strength and the fracture toughness values. In general, Wang et al[120] explained that increase in strength observed in ZrB_2 containing "nano-SiC whiskers" occurred due to the

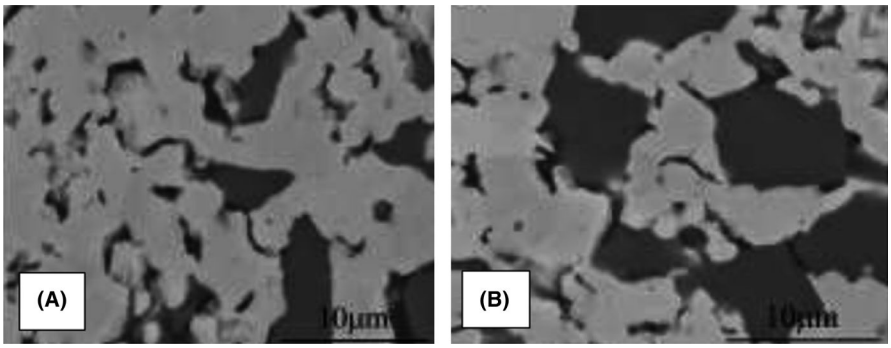

FIGURE 11 Microstructures of ZrB_2–SiC specimens for (A) 15% SiC and (B) 30% SiC[117]

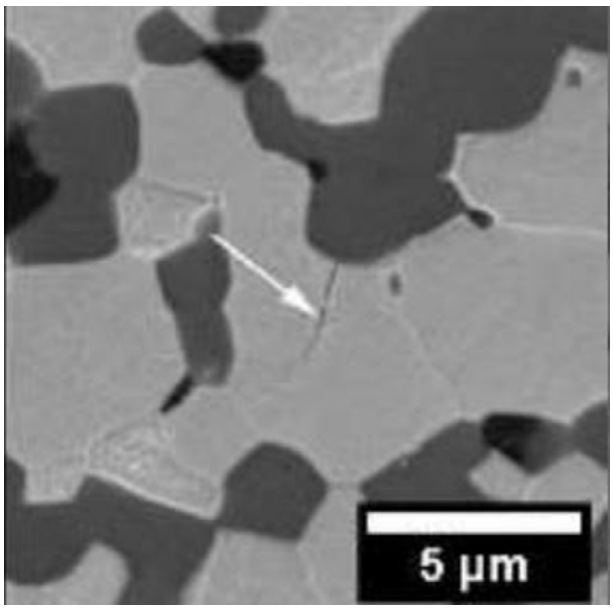

FIGURE 12 Microstructure of ZrB_2–SiC, with the presence of microcracks, due to large SiC clusters[119]

characteristics of the fine microstructure and the reinforcement action that the "nano-SiC whiskers" provided as shown in Figure 13. Whisker-toughening mechanisms are such as whisker pull-out, whisker bridging, and crack deflection in ceramic matrix composites. The fracture toughness of the composites increased Monteverde and Bellosi[121] processed ZrB_2 + α15SiC + 4.5ZrN (ZSZ) and ZrB_2 + 35HfB_2 + 10α-SiC + 4.5ZrN (ZHSZ) via hot press at 1900°C for 5 and 20 minutes, respectively. Microstructure revealed regularly faceted diborides grains with grain size distribution wider in ZSHZ composite (Figure 14) with hardness of 15.6 GPa and 16.7 GPa for ZSZ and ZHSZ composites, respectively. Summarizing, the correct amount of SiC provides benefits for oxidation resistance due to the formation of a protective borosilicate glass layer rich in SiO_2 and ablation resistance, without harming stability under high temperatures. Additionally, better hardness, longitudinal elasticity module, flexure strength, and fracture toughness are reported as discussed above when one has a fine grain size and a uniform distribution of the reinforcing phase.

6 | RELATION BETWEEN MECHANICAL PROPERTIES AND WEAR PERFORMANCE OF ZrB_2–SiC COMPOSITE

ZrB_2–SiC (UHTCs) are generally used in liquid propellant rocket motors, supersonic planes, space planes, turbojet parts, thermal structures for space planes and other space probes, gas turbines combustors cans, brakes, after burners, heat shields, prostheses, fixation plates, thermal insulation, or rocket nozzles etc, which undergo adhesive, abrasive, fatigue, or corrosion wear with time. So wear has a great role in long life functioning of these components as excessive wear of the mating components sometimes lead to catastrophic failure.[122–127] Literature survey revealed that wear

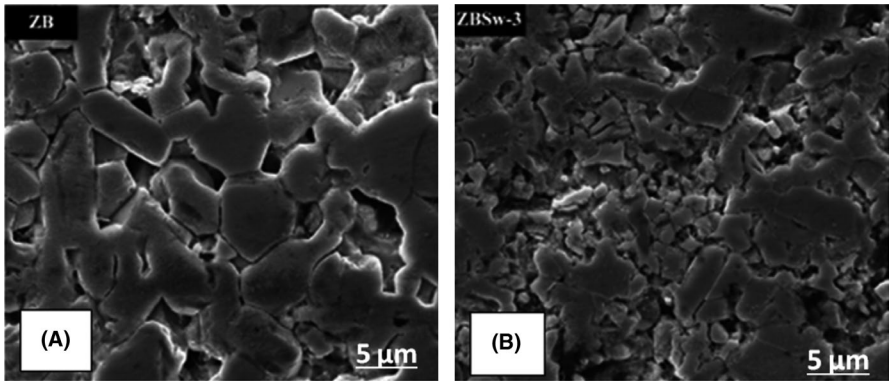

FIGURE 13 Scanning electron micrographs of ZrB_2–SiCw. ZB refers to (A) 100% ZrB_2, and (B) ZBSw-3 (85 vol% ZrB_2 + 15 vol% nano-SiC whiskers)[120]

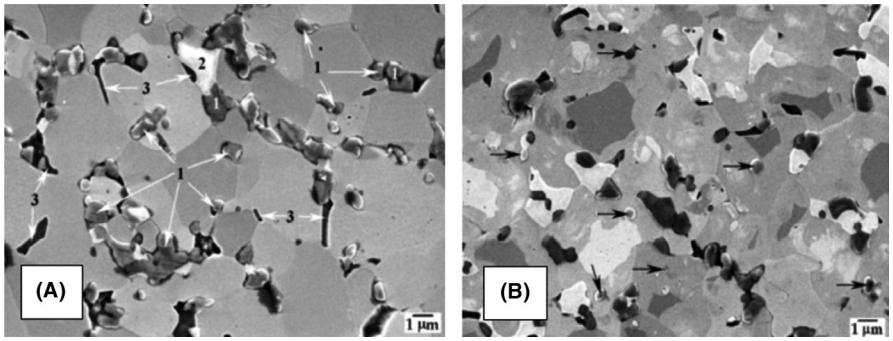

FIGURE 14 A, ZSZ composition microstructure. The numbers correspond to (1) SiC, (2) ZrO_2, and (3) BN; (B) ZSHZ-Black arrows denote intragranular SiC particulates[121]

TABLE 5 Physical and mechanical properties of ZrB_2-based ceramic composite

Composition	Processing Technique	Sintering Temp (°C)	Pressure (MPa)	Time (min)	Density (%)	Hardness (GPa)	Fracture toughness (MPa. $m^{1/2}$)	References
ZrB_2-(10-30 vol%)SiC	SPS	1600	55	2	98-100	18-23	4.2-5.3	[115]
ZrB_2	SPS	2100	35	25	98.65	16.64	4.69	[129]
ZrB_2–B_4C	SPS	1800-2050	50	10	99.1	19.02 ± 1.07	4.4 ± 0.27	[130]
ZrB_2–SiC	”	1800-2050	50	10	98.7	17.33 ± 1.23	4.47 ± 0.43	[130]
ZrB_2–ZrC	”	1800-2050	50	10	99.7	14.73 ± 1.12	5.26 ± 0.69	[130]
ZrB_2	Hot pressed	2100	40	120	97.30	14.72 ± 1.3	2.30 ± 0.22	[131]
ZrB_2-(5-15 wt%)B_4C	”	2100	40	120	89.53-95.28	18.03 ± 1.7-20.81 ± 1.6	2.95 ± 0.21-3.93 ± 0.22	[131]
ZrB_2	Hot pressed	2100	34.3	60	5.95 g/cm^3	16	4.2	[132]
ZrB_2–B_4C	”	2100	34.3	60	3.57 g/cm^3	—	—	[132]
ZrB_2–B_4C–SiC	”	2100	34.3	60	3.56 g/cm3	27	5.0	[132]
ZrB_2–SiC_P	Hot pressed	2200	50	120	93	17.72 ± 0.78	3.17 ± 0.13	[133]
ZrB_2–SiC_C	”	2200	50	120	92	19.13 ± 1.34	5.3 ± 0.27	[133]
ZrB_2–SiC_H	”	2200	50	120	91	17.55 ± 0.13	3.38 ± 0/38	[133]
B_4C-ZrB_2	”	1800	30	60	95.4	33 ± 2	3.6 ± 0.5	[134]
(5-60 vol%)ZrB_2–SiC	SPS	1600	35	30	84.6-99.1	7.42 ± 0.3-17.54 ± 0.9	4.99 ± 0.4-5.65 ± 0.6	[139]
ZrO_2-30 vol%ZrB_2	HIP	1400	110	60	97-100	~16	~17	[140]
AA6351-(3-9 wt%)ZrB_2	Furnace	850	-	30	-	46-115$Hv_{.5}$	-	[141]
ZrB_2-(0-30 wt%)TiB_2	Hot pressed	2200	50	120	95-99	14.40 ± 1.33 -22.34 ± 1.65	2.52 ± 0.13 -3.01 ± 0.19	[73]

TABLE 6 The summary of tribological behavior of ZrB_2-based ceramic composites worn against different counter bodies in dry conditions

Composition	Counter body	Wear (dry)	Load (N)	Velocity (m/s)	COF	Wear rate (mm^3/N.m)	Wear mechanism	References
ZrB_2-(10-30)SiC	SiC	Erosion wear	—	47	—	—	Fracture, grain pullouts	[115]
ZrB_2	-	Pulse current	10	-	0.44	1.01×10^{-3}	Scratch, cracks	[129]
ZrB_2–B_4C	SiC	sliding	5-50	0.1	~0.73-~0.7	$(1.09\text{-}1.42) \times 10^{-5}$	Abrasive grooves, cracks; Tribofilm at high load	[130]
ZrB_2–SiC	”	”	”	”	~0.62 ~ 0.63	$(6.15\text{-}7.5) \times 10^{-6}$	”	[130]
ZrB_2–ZrC	”	”	”	”	~0.67 ~ 0.68	$(6.15\text{-}7.3) \times 10^{-6}$	Abrasive grooves, limited cracks; Tribofilm at high load	[130]
ZrB_2	Diamond Tip	sliding	5-10	1×10^{-4}	0.55-0.69	$1.63\text{-}1.97 \times 10^{-3}$	Plastic deformation	[131]
ZrB_2–$5B_4C$	”	”	”	”	0.44-0.45	$0.63\text{-}0.74 \times 10^{-3}$	”	[131]
ZrB_2–$10B_4C$	”	”	”	”	0.40-0.40	$0.47\text{-}0.49 \times 10^{-3}$	”	[131]
ZrB_2–$15B_4C$	”	”	”	”	0.47-0.49	$2.65\text{-}3.12 \times 10^{-3}$	”	[131]
ZrB_2	Test material pin	”	7.8	1.5×10^{-3}	~0.9	$\sim 10^{-10}$	Fracture-broken	[132]
ZrB_2–B_4C	”	Sliding	”	”	~0.99	3.2×10^{-12}	Fracture	[132]
ZrB_2–$15B_4C$–SiC	”	”	”	”	~0.87	9×10^{-13}	No Fracture	[132]
ZrB_2–SiC_P	Diamond tip	Sliding	5	1×10^{-4}	0.47	0.9×10^{-3}	Scratch grooves, cracks, transgranular grain boundary fracture	[133]
ZrB_2–SiC_C	”	”	”	”	0.47	1.31×10^{-3}	”	[133]
ZrB_2–SiC_H	”	”	”	”	0.48	1.24×10^{-3}	”	[133]
B_4C-ZrB_2	WC-Co	Reciprocative sliding	”	10 Hz	0.24	25.5×10^{-6}	Severe abrasive grooves, grains pullout	[134]
B_4C-ZrB_2	”	”	10	”	0.15	29.01×10^{-6}	Mild abrasive grooves along with oxidation	[134]
B_4C–ZrB_2	”	”	20	”	0.15	38.14×10^{-6}	Pullout, mild abrasive grooves and tribooxidative layer	[134]
20ZrB_2–SiC	SiC	Sliding	10	0.3	—	—	Microcrack, abrasion	[138,139]
60ZrB_2–SiC	”	”	10	”	—	—	Transgranular fracture	[138,139]
ZrO_2-30ZrB_2	Steel	Fretting wear	2-10	8 Hz	0.47-0.81	$\sim 10^{-7}$- $\sim 10^{-8}$	Abrasion, spalling	[140]
AA 6351-(3-9) ZrB_2	Steel	Sliding wear	9.8	1	0.24-0.5	$0.2\text{-}1.3 \times 10^{-3}$	Abrasion, pits, cracks, ploughing	[141]
ZrB_2-(5-3)TiB_2	Diamond tip	Sliding	5-10	1×10^{-4}	0.315-0.532	1.21×10^{-3}- 26.9×10^{-3}	plastic deformation	[73]

performance of ZrB_2-based ceramics was studied by several researchers majorly in un lubricated (dry) conditions, wear of ceramics depend on several factors like surface roughness, contact geometry, microstructural features, grain sizes, mechanical properties, load, speed, temperature, duration, and environment.[115-116,128–134] Erosive wear behavior of spark plasma-sintered ZrB_2-(10-30 vol%) SiC composites against SiC erodent at varying angle of incidence (30°-90°) at room and high (800°C) temperature revealed that increased % of SiC resulted in 68% and 78% reduction in erosive wear rate of the composite at room and high temperature, respectively.[115] B_2O_3 and SiO_2 layer formation increased the high-temperature erosion resistance.[115] Tables 5 and 6 show the details of wear performance of ZrB_2-based ceramics having different mechanical properties and processed via different routes. SEM micrograph of scratch track of spark plasma sintered ZrB_2 by direct and pulse current under 10 N load are shown in Figure 15. Z Addition of SiC in ZrB_2–B_4C ceramic composite restricted fracture even at high friction in comparison to monolithic and ZrB_2–B_4C composite.[126] ZrB_2 ceramics processed with B_4C, SiC, and ZrC as additives undergo abrasive grooves and cracks at low loads and tribofilm formation due to oxidation due to wear at high load. ZrC addition has restricted the crack formation[135] (Figure 16).[130] There is not large variation observed in friction in all three composites, whereas B_4C addition resulted in highest wear rate at low and high load.[130] Study of addition of varying (5-15 wt%) of B_4C revealed low density with increasing wt% and high hardness and fracture toughness with 10 wt% B_4C addition. Least COF and wear was observed in ZrB_2–$10B_4C$ ceramic composite and crack deflections with B_4C addition has resulted in improved mechanical and wear properties.[131] Wear in water medium resulted in thermochemical degradation of monolithic ZrB_2 and least wear rate was noticed in ZrB_2–$15B_4C$–SiC composite.[132] SiC addition resulted in better bonding, contiguity with interconnected network with ZrB2, which imparts high mechanical and wear performance.[133] Debnath et al (2015)[133] processed ZrB_2-based ceramic composite by adding SiC (SiC_P, SiC_C, SiC_H) obtained from different sources: precursor (PCS derived SiC),[110,136,137]CUMI-M15, HC Starck-UF25. Highest density was found in ZrB_2–SiC_P composition whereas ZrB_2–SiC_C possess high hardness and fracture toughness. Transgranular lateral cracking, slip lines- and material removal was found in indentation and scratch grooves in all the composites and COF was also found low at all loads (5-10 N) [133]. Wear behaviour of ZrB_2–B_4C composite processed via reactive hot pressing of B_4C and ZrO_2 revealed decrease in COF with increasing load and less wear than monolithic B_4C.[134] Wear behavior of nanoscaled (20-60 vol%) ZrB_2–SiC (ZS) composites prepared via polymer derived route followed by SPS was studied by Jiabei et al (2018).[138,139] They found transition of wear mechanism from microcrack to abrasion with increasing wear time in 20 ZS whereas surface of 60 ZS was found stable with less debris formation during wear showing superior wear resistance[139] as shown in Figure 17A,B. Abrasion and spalling wear was found in ZrO_2–30 ZrB_2 composite in fretting wear and decreasing wear rate with increasing toughness of the composites.[140] Kumar et al (2009)[141] prepared AA6351-(3-9 wt%)ZrB_2 in situ composite by the

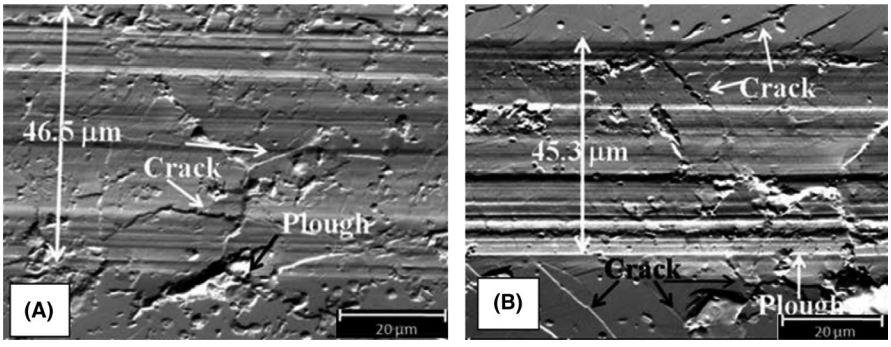

FIGURE 15 SEM micrograph of scratch track of spark plasma-sintered ZrB_2 by (A) direct current and (B) pulse current under 10 N load[129]

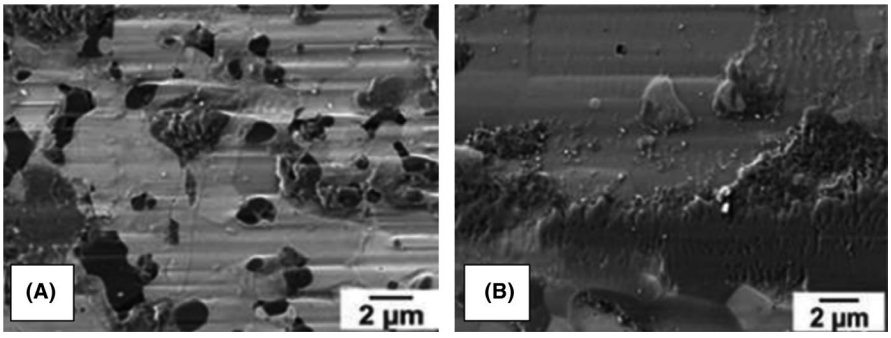

FIGURE 16 Wear tracks of (A) ZrB_2-10 wt% SiC and (B) ZrB_2-10 wt% ZrC at 50 N load[130]

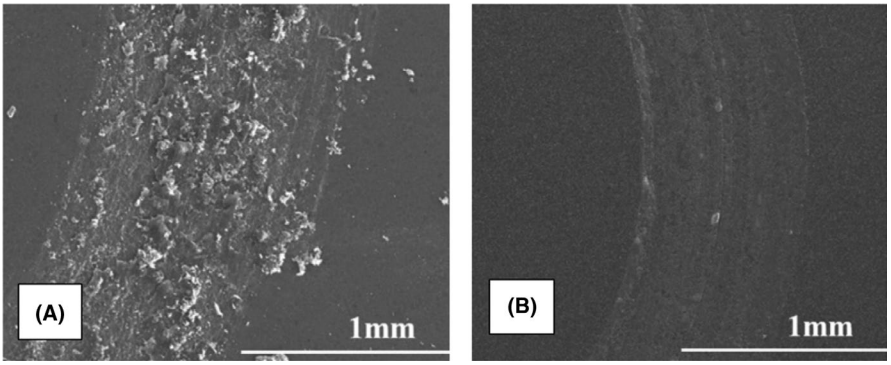

FIGURE 17 Surface morphologies of wear track after different distance tests (50 000 cycles) with 0.3 m radius under a load of 10 N (A) 20 ZS (B) 60 ZS[139]

reaction of K_2ZrF_6 and KBF_4 with molten aluminum alloy at 850°C. Pin on disc wear study of solutionized and solutionized-aged casted composites was done. Increased % of ZrB_2 in solutionized and solutionized-aged composites increased the hardness of the composite and adhesive wear mechanism was found dominant in all the composites whereas monolithic matrix was full of coarse and plastically deformed grooves.[141] Effect of addition of TiB_2 in ZrB_2 composites formed solid solution and improved mechanical and tribological performance. Increased weight of TiB_2 addition up to 30% led to high hardness, fracture toughness, and wear resistance. Worn surfaces were plastically deformed upon contact between test specimen and stylus.[73]

7 | CONCLUSION AND OUTLOOK

Summarizing, present paper gives a detailed systematic review of the research done on physical, mechanical and tribological performance of ZrB_2-based ceramic composites with or without additives processed via different routes and conditions. Study of ZrB_2–SiC ceramic composites resulted out excellent information about the variation in properties based on different sintering parameters. Fine particles dispersed in composite system resulting in more homogeneous dense structure. Present review revealed that large SiC grains in the microstructure act as critical flaw causing the specimen failure. It is expected to have improved properties of these composites by reinforcing them with nano phase of SiC. It is found that larger volume % of nanocrystalline SiC content gives much better performance than their counterpart conventional coarse-grained polycrystalline materials in respect of the grain boundary strengthening or fine-grain strengthening. Wear resistance of ZrB_2-based composite against erosive, sliding, or fretting wear make them more suitable for industrial use. Further research is clearly needed to use their potential applications under wide range of temperature and pressure encountered in aerospace, hypersonic flights, atmospheric re-entry, and rocket propulsion system.

ACKNOWLEDGMENT

The authors gratefully acknowledge the financial support of the Ministry of Science and Higher Education of the Russian Federation in the framework of Increase Competitiveness Program of NUST «MISiS» (№ K4-2018-020), *implemented by a governmental decree dated 16th of March 2013, N 211.*

ORCID

Vikas Verma https://orcid.org/0000-0002-9478-8278

REFERENCES

1. Bansal NP. Handbook of ceramic composites. Kluwer Academic Publishers, Boston/Dordrecht/London: Springer; 2005. p. 1–532.
2. Fahrenholtz WG, Hilmas GE, Talmy IG, Zaykoski JA. Refractory diborides of zirconium and hafnium. J Am Ceram Soc. 2007;90:1347–64.
3. Hulbert DM, Jiang D, Dudina DV, Amiya K. The synthesis and consolidation of hard materials by spark plasma sintering. Int J Refract Met Hard Mater. 2009;27:367–75.
4. Low IM, Sakka Y, Hu CF. Max phases and ultra-high temperature ceramics for extreme environments. Hershey, PA: IGI Global; 2013. p. 1–553.
5. Akin I, Hottab M, Sahina FC, Yucela O, Gollera G, Goto T. Microstructure and densification of ZrB_2–SiC composites prepared by spark plasma sintering. J Eur Ceram Soc. 2009;29:2379–85.
6. Verma V, Kumar BVM. Processing of TiCN–WC–Ni/Co Cermets via conventional and spark plasma sintering technique. Trans Indian Inst Met. 2017;70:843–53.
7. Loehman R, Corral E, Dumm HP, Kotula P, Tandon R. Ultra high temperature ceramics for hypersonic vehicle applications ronald. Sandia Report. Sandia National Laboratories Albuquerque, New Mexico 87185 and Livermore, California 945502006. 2006;1–46.
8. Alfano D. Spectroscopic properties of carbon fibre reinforced silicon carbide composites for aerospace applications, source: properties and applications of silicon carbide. IntechOpen. 2011;231–50.
9. Fahrenholtz WG, Hilmas GE. An introduction to ultra-high temperature ceramics. Manchester: AZO Materials; 2010. p. 1–6.
10. Eakins E, Jayaseelan DD, Lee WE. Toward oxidation-resistant ZrB_2-SiC ultra high temperature ceramics. Min Met Mater Soc ASM Int. 2011;42A:878–87.

11. Fahrenholtz WG, Wuchina EJ, Lee WE, Zhou Y. Ultra-high temperature ceramics: materials for extreme environment applications. J Am Ceram Soc; 2014; 1: 1–441.
12. Monteverde F, Bellosi A, Scatteia L. Processing and properties of ultra-high temperature ceramics for space applications. Mater Sci Eng A. 2008;485:415–21.
13. Bilal A, Jahan MP, Talamona D, Perveen A. Electro-discharge machining of ceramics: a review. Micromachines. 2019;10:1–41.
14. Savino R, De Stefano Fumo M, Paterna D, Serpico M. Aerothermodynamic study of UHTC-based thermal protection systems. Aero Sci Tech. 2005;9:151–60.
15. Wuchina E, Opila E, Opeka M, Fahrenholtz W, Talmy I. UHTCs: Ultra-high temperature ceramic materials for extreme environment applications. Electrochem Soc Interface. 2007; 16: 30–6.
16. Fahrenholtz WG, Hilmas GE, Warts J, Thompson M, Teague M, Chamberlain A, et al. Design of ultra-high temperature ceramics for improved performance. Report: AFRL-SR-AR-TR-09-0038; 2009:1–47.
17. Chamberlain A, Fahrenholtz WG, Hilmas GE, Ellerby D. Oxidation of ZrB_2 under atmospheric and reentry conditions. Refrac App Transac. 2005;1:1–7.
18. Johnson SM, Gash M, Lawson JW, Gusman MI, Stackpoole MM. Recent Developments in ultra high temperature ceramics at NASA Ames. 16th AIAA/DLR/DGLR International Space Planes and Hypersonic Systems and Technologies Conference, 2009; p. 1–10.
19. Johnson S. Ultra High. High temperature ceramics: application, issues and prospects, 2nd edn. Baltimore, MD: Ceramic Leadership Summit; 2011.
20. Justin JF, Jankowiak A. Ultra high temperature ceramics: densification, properties and thermal stability. J AerospaceLab. 2011;3:1–11.
21. Levinea SR, Opilab EJ, Halbig MC, Kiser JD, Singh M, Salem JA. Evaluation of ultra-high temperature ceramics for aeropropulsion use. J Eur Ceram Soc. 2002;22:2757–67.
22. Zimmermann JW, Hilmas GE, Fahrenholtz WG. Thermal shock resistance and fracture behavior of zrb_2–based fibrous monolith ceramics. J Am Ceram Soc. 2009;92:161–6.
23. Izhevskyi VA, Genova LA, Bressiani JC, Bressiani AHA. Review article: silicon carbide. structure, properties and processing. Ceramica. 2000;46(297):4–13.
24. Hu P, Guolin W, Wang Z. Oxidation mechanism and resistance of ZrB_2–SiC composites. Corr Sci. 2009;51:2724–32.
25. Kelly JF, Fisher GR, Barnes P. Correlation between layer thickness and periodicity of long polytypes in silicon carbide. Mat Res Bulletin. 2005;40:249–55.
26. Laine RM, Babonneau F. Preceramic polymer routes to silicon carbide. Chem Mater. 1993;5:260–79.
27. Kumar BVM, Kim YW, Lim DS, Seo WS. Influence of small amount of sintering additives on unlubricated sliding wear properties of SiC ceramics. Ceram Int. 2011;37:3599–608.
28. Roewer G, Herzog U, Trommer K, Muller E, Fruhauf S. Silicon carbide - a survey of synthetic approaches, properties and applications. Struc Bond. 2002;101:59–135.
29. Monteverde F. Ultra-high temperature HfB_2–SiC ceramics consolidated by hot pressing and spark plasma sintering. J Alloys Comp. 2007;428:197–205.
30. Fahrenholtz WG. Thermodynamic analysis of ZrB_2–SiC oxidation: formation of a SiC-depleted region. J Am Ceram Soc. 2007;90:143–8.
31. Jung EY, Kim JH, Jung SH, Choi SC. Synthesis of ZrB^2 powders by carbothermal and borothermal reduction. J Alloys Comp. 2012;538:164–8.
32. Guo WM, Zhang GJ. Reaction processes and characterization of zrb_2 powder prepared by boro/carbothermal reduction of ZrO^2 in vacuum. J Am Ceram Soc. 2009;92:264–7.
33. Rezaie A, Fahrenholtz WG, Hilmas GE. Effect of hot pressing time and temperature on the microstructure and mechanical properties of ZrB_2-SiC. J Mater Sc. 2007;42:2735–44.
34. Chamberlain AL, Fahrenholtz WG, Hilmas GE, Ellerby DT. Characterization of zirconium diboride for thermal protection systems. Key Eng Mat. 2004;264–268:493–6.
35. Wang HL, Wang C. Preparation and mechanical properties of laminated zirconium diboride/molybdenum composites sintered by spark plasma sintering. Front Mater Sci China. 2009;3:273–80.
36. Venkateswaran T, Basu B, Raju GB, Kim DY. Densification and properties of transition metal borides-based cermets via spark plasma sintering. J Eur Ceram Soc. 2006;26:2431–40.
37. Clougherty EV, Wilkes KE, Tye RP. Research and development of refractory oxidation-resistant diborides, Technical Report AFML-TR-88-190, Part II, Volume V: thermal, physical, electrical and optical properties, ManLabs Inc; 1969:1–81.
38. Sciti D, Balbo A, Bellosi A. Oxidation behaviour of a pressureless sintered HfB_2–$MoSi_2$ composite. J Eur Ceram Soc. 2009;29:1809–15.
39. Bergero L, Sglavo VM, Soraru GD. Processing and thermal shock resistance of a polymer-derived $MoSi_2$/SiCO ceramic composite. J Am Ceram Soc. 2005;88:3222–5.
40. Chamberlain AL, Fahrenholtz WG, Hilmas GE. Pressureless sintering of zirconium diboride. J Am Ceram Soc. 2006;89:450–6.
41. Khanra AK, Pathak LC, Mishra SK, Godkhindi MM. Self-propagating-high-temperature synthesis (SHS) of ultrafine ZrB_2 powder. J Mat Sci. Lett. 2003;22:1189–91.
42. Chamberlain AL, Fahrenholtz WG, Hilmas GE. Reactive hot pressing of zirconium diborides. J Eur Ceram Soc. 2009;29:3401–8.
43. Nishiyama K, Nakamur T, Utsumi S, Sakai H, Abe M. Preparation of ultrafine boride powders by metallothermic reduction method. J Phys: Conf Ser. 2009;176:1–8.
44. Zhu S, Fahrenholtz WG, Hilmas GE. Enhanced densification and mechanical properties of ZrB_2–SiC processed by a preceramic polymer coating route. Scrip Mater. 2008;59:123–6.
45. Zhang SC, Hilmas GE, Fahrenholtz WG. Mechanical properties of sintered ZrB_2-SiC ceramics. J Eur Ceram Soc. 2011;31:893–901.
46. Fahrenholtz WG. Thermodynamic analysis of ZrB_2-SiC oxidation: formation of a SiC-depleted region. J Am Ceram Soc. 2007;90:143–8.
47. Speyer RF. Oxidation resistance, electrical and thermal conductivity, and spectral emittance of fully dense HfB_2 and ZrB_2 with SiC, $TaSi_2$, and LaB_6 Additives, Report: AFRL-OSR-VA-TR-2012-0279. 2012:4–99.
48. Lawson JW, Bauschlicher Jr CW, Daw MS. Ab initio computations of electronic, mechanical, and thermal properties of ZrB_2 and HfB_2. J Am Ceram Soc. 2011;94:3494–9.
49. Basu B, Balani K. Advanced structural ceramics. Hoboken, NJ: The American Ceramic Society, A John Wiley & Sons, Inc.; 2011. p. 1–504.
50. Vaßen R, Stover D. Processing and properties of nano phase non-oxide ceramics. Mat Sci Eng. 2001;A301:59–68.

51. Zhang Y, Gao D, Xu C, Song Y, Shi X. Oxidation behavior of hot pressed ZrB_2-ZrC-SiC ceramic composites. Int J Appl Ceram Technol. 2013;1–8.
52. Hu P, Wang Z. Flexural strength and fracture behavior of ZrB_2–SiC ultra-high temperature ceramic composites at 1800°C. J Eur Ceram Soc. 2010;30:1021–6.
53. Zhang GJ, Guo WM, Ni DW, Kan YM. Ultrahigh temperature ceramics (UHTCs) based on ZrB_2 and HfB_2 systems: powder synthesis, densification and mechanical Properties. J Phy.: Conference Series. 2009;012041176:1–12.
54. Licheri R, Orru R, Musa C, Locci AM, Cao G. Spark plasma sintering of ZrB_2-and HfB_2-based UHTCs prepared by SHS. Int J Self Prop High Temp Syn. 2009;18:15–24.
55. Lomello F, Bonnefont G, Leconte Y, Boime NH, Fantozzi G. Processing of nano-SiC ceramics: densification by SPS and mechanical characterization. J Eur Ceram Soc. 2012;32:633–41.
56. Zhu S, Fahrenholtz WG, Hilmas HE. Influence of silicon carbide particle size on the microstructure and mechanical properties of zirconium diboride–silicon carbide ceramics. J Eur Ceram Soc. 2007;27:2077–83.
57. Asl MS, Kakroudi MG. Characterization of hot-pressed graphene reinforced ZrB_2-SiC composite. Mater Sci Eng A. 2015;625:385–92.
58. Yadhukulakrishnan GB, Rahman A, Karumuri S, Stackpoole MM, Kalkan AK, Singh RP, et al. Spark plasma sintering of silicon carbide and multi-walled carbon nanotube reinforced zirconium diboride ceramic composite. Mater Sci Eng A. 2012;552:25–133.
59. Zhu X, Tang F, Suzuki TS, Sakka Y. Role of the initial degree of ionization of polyethylenimine in the dispersion of silicon carbide nanoparticles. J Am Ceram Soc. 2003;86:189–91.
60. Nisar A, Ariharan S, Venkateswaran T, Sreenivas N, Balani K. Effect of carbon nanotube on processing, microstructural, mechanical and ablation behavior of ZrB_2 -20SiC based ultrahigh temperature ceramic composites. Carbon. 2017;111:269–82.
61. Zhang H, Yan Y, Huang Z, Liu X, Jiang D. Pressureless Sintering of ZrB_2-SiC ceramics incorporating sol-gel synthesized ultra-fine ceramic powders. Key Eng Mat. 2010;434–435:193–6.
62. Patel M, Reddya JJ, Prasad VVB, Jayaram V. Strength of hot pressed ZrB_2–SiC composite after exposure to high temperatures (1000–1700°C). J Eur Ceram Soc. 2012;32:4455–67.
63. Rangaraj L, Suresha SJ, Divakar C, Jayaram V. Low temperature processing of ZrB_2-ZrC composites by reactive hot pressing. Min Met Mat Soc. ASM Int. 2008;39A:1496–505.
64. Rangaraj L, Divakar C, Jayaram V. Reactive hot pressing of ZrB_2–ZrCx ultra-high temperature ceramic composites with the addition of SiC particulate. J Eur Ceram Soc. 2010;30:3263–6.
65. Nasiri Z, Mashhadi M, Abdollahi A. Effect of short carbon fiber addition on pressureless densification and mechanical properties of ZrB_2–SiC–C_{sf} nanocomposite. Int J Refrac Met Hard Mater. 2015;51:216–23.
66. Nisar A, Khan MDM, Bajpai S, Balani K. Processing, microstructure and mechanical properties of HfB_2-ZrB_2-SiC composites: effect of B_4C and carbon nanotube reinforcement. Int J Refract Met Hard Mater. 2019;81:111–8.
67. Bellosi A, Monteverde F, Sciti D. Fast densification of ultra-high-temperature ceramics by spark plasma sintering. Int J App Ceram Tech. 2006;3:32–40.
68. Zamora V, Ortiz AL, Guiberteau F, Nygren M. On the enhancement of the spark-plasma sintering kinetics of ZrB_2–SiC powder mixtures subjected to high-energy co-ball-milling. Ceram Int. 2013;39:4191–204.
69. Zamora V, Ortiz AL, Guiberteau F, Nygren M. Spark-plasma sintering of ZrB_2 ultra-high-temperature ceramics at lower temperature via nanoscale crystal refinement. J Eur Ceram Soc. 2012;32:2529–36.
70. Sciti D, Silvestroni L. Processing, sintering and oxidation behavior of SiC fibers reinforced ZrB_2 composites. J Eur Ceram Soc. 2012;32:1933–40.
71. Rezaie A, Fahrenholtz WG, Hilmas GE. Evolution of structure during the oxidation of zirconium diboride–silicon carbide in air up to 1500°C. J Eur Ceram Soc. 2007;27:2495–501.
72. Jia L, Xinghong Z, Zhi W, Wenbo H. Microstructure and mechanical properties of ZrB_2–SiC–ZrO_{2f} ceramic. Scr Mater. 2011;64:872–5.
73. Chakraborty S, Debnath D, Mallick AR, Das PK. Mechanical and thermal properties of hot pressed ZrB_2 system with TiB_2. Int J Refrac Met Hard Mater. 2014;46:35–42.
74. Hassan R, Omar S, Balani K. Solid solutioning in ZrB_2 with HfB_2: effect on densification and oxidation resistance. Int J Refrac Met Hard Mater. 2019;84:105041.
75. Nisar A, Khan MDM, Balani K. Enhanced thermo-mechanical damage tolerance of functionally graded ZrB_2-20SiC ceramic reinforced with carbon nanotube. Ceram Int. 2019;45:6198–208.
76. Nisar A, Balani K. Phase and microstructural correlation of spark plasma sintered HfB_2-ZrB_2 based ultra-high temperature ceramic composites. Coatings. 2017;7:110–5.
77. Monteverde F, Guicciardi S, Bellosi A. Advances in microstructure and mechanical properties of zirconium diboride based ceramics. Mat Sci Eng A. 2003;346:310–9.
78. Zoli L, Vinci A, Silvestroni L, Sciti D, Reece M, Grasso S. Rapid spark plasma sintering to produce dense UHTCs reinforced with undamaged carbon fibres. Mater Des. 2017;130:1–7.
79. Asl MS, Nayebi B, Shokouhimehr M. TEM characterization of spark plasma sintered ZrB_2 –SiC–graphene nanocomposite. Ceram Int. 2018;44:15269–73.
80. Zhou S, Wang Z, Zhang W. Effect of graphite flake orientation on microstructure and mechanical properties of ZrB_2–SiC–graphite composite. J Alloys Comp. 2009;485:181–5.
81. Yadhukulakrishnan GB, Karumuri S, Rahman A, Singh RP, Kalkan AK, Harimkar SP. Spark plasma sintering of graphene reinforced zirconium diboride ultra-high temperature ceramic composites. Ceram Int. 2013;39:6637–46.
82. Zhang X, An Y, Han J, Han W, Zhao G, Jin X. Graphene nanosheet reinforced ZrB_2–SiC ceramic composite by thermal reduction of graphene oxide. RSC Adv. 2015;5:47060–5.
83. Binner J, Porter M, Baker B, Zou JI, Venkatachalam V, Diaz VR, et al. Selection, processing, properties and applications of ultra-high temperature ceramic matrix composites, UHTCMCs – a review. Int Mat Rev. 2019;1–57.
84. Cheng Y, Hu P, Zhou S, Zhang X, Han W. Using macroporous graphene networks to toughen ZrC–SiC ceramic. J Eur Ceram Soc. 2018;38:3752–8.
85. Yadhukulakrishnan GB, Rahman A, Karumuri S, Stackpoole MM, Kalkan AK, Singh RP, et al. Spark plasma sintering of silicon carbide and multi-walled carbon nanotube, reinforced zirconium diboride ceramic composite. Mater Sci Eng A. 2012;552:125–33.
86. Asl MS, Farahbakhsh I, Nayebi B. Characteristics of multi-walled carbon nanotube toughened ZrB_2-SiC ceramic composite prepared by hot pressing. Ceram Int. 2016;42:1950–8.

87. Lin J, Huang Y, Zhang H, Yang Y, Li N. Microstructure and mechanical properties of spark plasma sintered ZrB2–SiC–MWCNT composites. Ceram Int. 2015;41:15261–5.
88. Zimmermann JW, Hilmas GE, Fahrenholtz WG, Monteverde F, Bellosi A. Fabrication and properties of reactively hot pressed ZrB_2–SiC ceramics. J Am Ceram Soc. 2007;27:2729–36.
89. Zhou XJ, Zhang GJ, Li YG, Kan YM, Wang PL. Hot pressed ZrB_2–SiC–C ultra high temperature ceramics with polycarbosilane as a precursor. Mater Lett. 2007;61:960–3.
90. Wang Y, Zhu M, Cheng L, Zhang L. Fabrication of SiC_w reinforced ZrB_2-based ceramics. Ceram Int. 2010;36:1787–90.
91. Hu H, Wang Q, Chen Z, Zhang C, Zhang Y, Wang J. Preparation and characterization of C/SiC–ZrB_2 composites by precursor infiltration and pyrolysis process. Ceram Int. 2010;36:1011–6.
92. Kim Y, Jang H, Kim DJ. Enhanced sintering of SiC using infiltration of preceramic polymer. Ceram Int. 2011;37:2957–61.
93. Guron MM, Kim MJ, Sneddon LG. A simple polymeric precursor strategy for the syntheses of complex zirco and hafnium-based ultra high-temperature silicon-carbide composite ceramics. J Am Ceram Soc. 2008;91:1412–5.
94. Soraru GD, Pederiva L, Latournerie J, Raj R. Pyrolysis kinetics for the conversion of a polymer into an amorphous silicon oxycarbide ceramic. J Am Ceram Soc. 2002;85:2181–7.
95. Rouxel T, Sangleboeuf JC, Guin JP, Keryvin V, Soraru GD. Surface damage resistance of gel-derived oxycarbide glasses: hardness, toughness, and scratchability. J Am Ceram Soc. 2001;84:2220–4.
96. Varga T, Navrotsky A, Moats JL, Morcos RM, Poli F, Muller K, et al. Thermodynamically stable $Si_xO_yC_z$ polymer-like amorphous ceramics. J Am Ceram Soc. 2007;90:3213–9.
97. Kumar BVM, Kim YW. Processing of polysiloxane-derived porous ceramics: a review. Sci Tech Adv Mater. 2010;11:1–16.
98. Liu J, Zhang L, Liu Q, Cheng L, Wang Y. Polymer-derived SiOC–barium–strontium aluminosilicate coatings as an environmental barrier for C/SiC composites. J Am Ceram Soc. 2010;93:4148–52.
99. Eom JH, Kim YW, Jung BJ. Effect of alkaline earth additives on the flexural strength of silicon oxycarbide-bonded silicon carbide ceramics. Ceram Int. 2013;39:2083–91.
100. Kim YW, Kim SH, Song I, Kim HD, Park CB. Fabrication of open-cell, microcellular silicon carbide ceramics by carbothermal reduction. J Am Ceram Soc. 2005;88:2949–51.
101. Soraru GD, Modena S, Guadagnino E, Colombo P, Egan J, Pantano C. Chemical durability of silicon oxycarbide glasses. J Am Ceram Soc. 2002;85:1529–36.
102. Soraru GD, Campostrini R, Maurina S, Babonneau F. Gel precursor to silicon oxycarbide glasses with ultrahigh ceramic yield. J Am Ceram Soc. 1997;80:999–1004.
103. Xu T, Ma Q, Chen Z. High-temperature behavior of silicon oxycarbide glasses in air environment. Ceram Int. 2011;37:2555–9.
104. Eom JH, Kim YW. Low-temperature processing of silicon oxycarbide-bonded silicon carbide. J Am Ceram Soc. 2010;93:2463–6.
105. Kim JY, Kim YW, Mitomo M, Zhan GD, Lee JG. Microstructure and mechanical properties of a silicon carbide sintered with yttrium–aluminum garnet and silica. J Am Ceram Soc. 1999;82:441–4.
106. Esfehanian M, Oberacker R, Fett T, Hoffmann MJ. Development of dense filler-free polymer-derived SiOC ceramics by field-assisted sintering. J Am Ceram Soc. 2008;91:3803–5.
107. Colombo P, Hellmann JR, Shelleman DL. Thermal shock behavior of silicon oxycarbide foams. J Am Ceram Soc. 2002;85:2306–12.
108. Harshea R, Balanb C, Riedela R. Amorphous Si(Al)OC ceramic from polysiloxanes bulk ceramic processing, crystallization behavior and applications. J Euro Ceram Soc. 2004;24:3471–82.
109. Colombo P, Mera G, Riedel R, Soraru GD. Polymer-derived ceramics: 40 years of research and innovation in advanced ceramics. J Am Ceram Soc. 2010;93:1805–37.
110. Toma L, Fasel C, Lauterbach S, Kleebe HJ, Ried R. Influence of nano-aluminum filler on the microstructure of SiOC ceramics. J Eur Ceram Soc. 2011;31:1779–89.
111. Zhang X, Hou Y, Hu P, Han W, Luo J. Dispersion and co-dispersion of ZrB_2 and SiC nano powders in ethanol. Ceram Int. 2012;38:2733–41.
112. Lee SH, Sakka Y, Kagawa Y. Dispersion behavior of ZrB_2 powder in aqueous solution. J Am Ceram Soc. 2007;90:3455–9.
113. Lu Z, Jiang D, Zhang J, Lin Q. Aqueous tape casting of zirconium diborides. J Am Ceram Soc. 2009;92:2212–7.
114. Huang T, Hilmas GE, Fahrenholtz WG, Leu MC. Dispersion of zirconium diboride in an aqueous, high-solids paste. Int J Appl Ceram Tech. 2007;4:470–9.
115. Gupta Y, Venkateswaran T, Kumar BVM. Influence of angle of incidence, temperature and SiC content on erosive wear behavior of ZrB_2-SiC composites. Int J App Ceram Tech. 2019;17:1–9.
116. Kumar Sharma S, Yashpal S, Selokar AW, Kumar BVM, Venkateswaran T. High temperature erosion behavior of spark plasma sintered ZrB_2-SiC composites. Ceram Int. 2017;43:8982–8.
117. Zhang X, Liu R, Xiong X, Chen Z. Mechanical properties and ablation behavior of ZrB_2–SiC ceramics fabricated by spark plasma sintering. Int J Refrac Met Hard Mater. 2015;48:120–5.
118. Zhang L, Kurokawa K. Effect of SiC addition on oxidation behavior of ZrB_2 at 1273 K and 1473K. Oxid Met. 1473K;85:311–20.
119. Neuman EW, Hilmas GE, Fahrenholtz WG. Mechanical behavior of zirconium diboride–silicon carbide ceramics at elevated temperature in air. J Eur Ceram Soc. 2013;33:2889–99.
120. Wang H, Wang CA, Yao X, Fang D. Processing and mechanical properties of zirconium diboride-based ceramics prepared by spark plasma sintering. J Am Ceram Soc. 2007;90:1992–7.
121. Monteverde F, Bellosi A. Development and characterization of metal-diboride-based composites toughened with ultra-fine SiC particulates. Solid State Sci. 2005;7:622–30.
122. Hsu SM, Shen M. Wear prediction of ceramics. Wear. 2004;256:867–78.
123. Bhushan B. Modern tribology handbook Vol I principle of tribology. New York Washington, D.C.: CRC Press LLC; 2017:1–28.
124. Kim SS, Kato K, Hokkirigawa K, Abe H. Wear mechanism of ceramic materials in dry rolling friction. Transac. ASME. 1986;522–6.
125. Adachi K, Kato K, Chen N. Wear map of ceramics. Wear. 1997;203–204:291–301.
126. Hsu SM, Shen MC. Ceramic wear maps. Wear. 1996;200:154–75.
127. Archard JF. The temperature of rubbing surfaces. Wear. 1959;2:438–55.
128. Opeka MM, Talmy IG, Wuchina EJ, Zaykoski JA, Causey SJ. Mechanical, thermal, and oxidation properties of refractory hafnium and zirconium compounds. J Eur Ceram Soc. 1999;19:2405–14.
129. Chakraborty S, Mallick AR, Debnath D, Das PK. Densification, mechanical and tribological properties of ZrB_2 by SPS: effect of pulsed current. Int J Refract Met Hard Mater. 2015;48:150–6.

130. Medveď D, Balko J, Sedlák R, Kovalčíková A, Shepa I, Naughton-Duszová A, et al. Wear resistance of ZrB_2 based ceramic composites. Int J Refract Met Hard Mater. 2019;81:214–24.
131. Chakraborty S, Debnath D, Mallick AR, Das PK. Mechanical, tribological, and thermal properties of hot-pressed ZrB_2-B_4C composite. Int J Appl Ceram Technol. 2014:1–9.
132. Umeda K, Enomoto Y, Mitsui A, Mannami K. Friction and wear of boride ceramics in air and water. Wear. 1993;169:63–8.
133. Debnath D, Chakraborty S, Mallick AR, Gupta RK, Ranjan A, Das PK. Mechanical, tribological and thermal properties of hot pressed ZrB_2–SiC composite with SiC of different morphology. Adv Appl Ceram. 2015;114:45–54.
134. Murthy Ch TSR, Ankata S, Sonber JK, Sairam K, Singh K, Nagara A, et al. Microstructure, thermo-physical, mechanical and wear properties of in-situ formed boron carbide – zirconium diboride composite. Ceram Silikaty. 2018;62:15–30.
135. Shiro S. A thermoanalytical study on the oxidation of ZrC and HfC powders with formation of carbon. Solid State Ionics. 2002;149:319–26.
136. Ionescu E, Papendorf B, Kleebe HJ, Riedel R. Polymer-derived silicon oxycarbide/hafnia ceramic nanocomposites. Part II: stability toward decomposition and microstructure evolution at T >>10001C. J Am Ceram Soc. 2010;93:1783–9.
137. Ionescu E, Papendorf B, Kleebe HJ, Poli F, Muller K, Riedel R. Polymer derived silicon oxycarbide/hafnia ceramic nanocomposites. Part I: phase and microstructure evolution during the ceramization process. J Am Ceram Soc. 2010;93:1774–82.
138. He J, Cao Y, Zhang Y, Wang Y. Mechanical properties of ZrB_2–SiC ceramics prepared by polymeric precursor route. Ceram Int. 2018;44:6520–6.
139. He J, Cao Y, Li Z, Wang Y. Study of tribological properties of polymer derived ZrB_2-SiC ceramics. Ceram Int. 2018;44:15627–30.
140. Bakshi SD, Basu B, Mishra SK. Fretting wear properties of sinter-HIPed ZrO_2–ZrB_2 composites. Comp: Part A. 2006;37:1652–9.
141. Kumar GN, Narayanasamy R, Natarajan S, Babu SPK, Sivaprasad K, Sivasankaran S. Dry sliding wear behaviour of AA 6351-ZrB_2 in situ composite at room temperature. Mater Design. 2010;31:1526–32.
142. Rangaraj L, Divakar C, Jayaram V. Fabrication and mechanisms of densification of ZrB2-based ultra high temperature ceramics by reactive hot pressing. J Eur Ceram Soc. 2010;30:129–38.
143. Tian WB, Kan YM,Zhang GJ, Wang PL. Effect of carbon nanotubes on the properties of ZrB2–SiC ceramics. Mater Sci Eng A. 2008;487:568–73.

How to cite this article: Verma V, Cheverikin V, Cozza RC. Review: Effect on physical, mechanical, and wear performance of ZrB_2-based composites processed with or without additives. *Int J Appl Ceram Technol*. 2020;17:2509–2532. https://doi.org/10.1111/ijac.13567